Received January 9, 2019, accepted January 25, 2019, date of publication January 31, 2019, date of current version February 14, 2019.

Digital Object Identifier 10.1109/ACCESS.2019.2896656

Minimal Realizations of Autonomous Chaotic Oscillators Based on Trans-Immittance Filters

JIRI PETRZELA AND LADISLAV POLAK, (Member, IEEE)
Department of Radio Electronics, SIX Research Center, Brno University of Technology, Technicka 3082/12, 61600 Brno, Czech Republic

Corresponding author: Ladislav Polak (polakl@feec.vutbr.cz)

Research described in this paper was financed by Czech Ministry of Education in frame of National Sustainability Program under grant LO1401. For research, infrastructure of the SIX Center was used.

ABSTRACT This review paper describes a design process toward fully analog realizations of chaotic dynamics that can be considered canonical (minimum number of the circuit elements), robust (exhibit structurally stable strange attractors), and novel. Each autonomous chaotic lumped circuit proposed in this paper can be understood as a looped system, where linear trans-immittance frequency filter interacts with an active nonlinear two-port. The existence of chaos is demonstrated via well-established numerical algorithms that represent the current standard in the field of nonlinear dynamics, i.e., by calculation of the largest Lyapunov exponent and high-resolution 1-D bifurcation diagrams. The achieved numerical results are put into the context of experimental measurement; observed state trajectories prove a one-to-one correspondence between theoretical expectations and practical outputs, i.e., prescribed strange attractors do not represent the chaotic transients. Finally, short term unpredictability of the chaotic flow is demonstrated via calculation of Kaplan–Yorke dimension that is high, i.e., generated waveforms can find interesting applications in the fields of chaotic masking, modulation, or chaos-based cryptography.

INDEX TERMS Analog oscillator, filtering two-port, chaos, immittance function, Lyapunov exponents, nonlinear dynamics, strange attractors.

I. INTRODUCTION

It is well known that chaos belongs to universal phenomena that can be observed in integer-order autonomous (isolated system, no driving forces) deterministic (without stochastic term) dynamical systems under two basic conditions: at least three degrees of freedom and an intrinsic nonlinearity. At the first sight, chaos seems to be noise-like dynamical behavior that can be predicted neither for long nor toward short future. It is also a kind of motion that is extremely sensitive to the changes of the initial conditions, produce dense state space attractors with fractal (non-integer) metric dimension and the generated waveforms have broad-band continuous frequency spectrum typically in the shape of a Gaussian-like distribution. Non-existence of a closed-form analytic solution, the so-called long-term unpredictability, is caused due to the exponential divergence of the neighboring state trajectories. On the other hand, formed strange attractors are bounded into a finite state space volume and prevent certain degree of structural stability. It means that chaotic systems are implementable as the lumped electronic circuits and chaotic attractors are observable using oscilloscope and real-time measurement. Unique properties of continuous-time chaotic signals mentioned above suggest possibilities for practical applications; see [1]–[3] for few examples.

Coming from pure numerical analysis of dimension-less state equations chaos can be observed in terms of dynamics of mathematical models that represents completely different physical, natural or artificial subject. Hence, factual meaning of individual state variables and internal system parameters is no longer relevant. Thanks to the arbitrary scaling factor also time (frequency) context is no longer important; both slow and fast chaotic transients can exhibit the same fingerprints.

Chaos has been firstly noticed and officially reported by Lorenz [4] during numerical study of a simplified mathematical model of wind circulation and, after publication of this break-through discovery in famous paper, researchers along the world started intensively look after algebraically simplest chaotic flows. Consequently, examples of chaotic dynamics were reported in chemistry as motion associated with simple chemical reactions [5]–[7]. Another example is deterministic chaos coming as the result of coupling chemical

The associate editor coordinating the review of this manuscript and approving it for publication was Ludovico Minati.

oscillators [8], [9]. Papers mentioned above are focused on analysis of the mathematical models that eventually turns to be aperiodic and/or chaotic. However, a real situation sometimes requires chaos to be stabilized. Example of the chaos control is provided in [10]. Turbulent dynamics in chemical reaction is described in [11] and turbulence in general is considered in [12]. Non-equilibrium thermodynamics with footprints of chaos is a topic of the paper [13]. Excellent examples of potentially chaotic systems are mechanical oscillators. Early manuscripts were aimed on simple models describing Newtonian dynamics [14]–[17], object movement [18], etc. Unpredictable time evolutions were confirmed also in the case of simple mathematical models that describe biological populations [19], [20]. List of chaotic dynamical systems continues with papers covering complex behavior of fluids [21], models describing fluid elastic vibrations [22], hydrodynamics [23], etc. Interestingly chaos was recognized within dynamics of mathematical models dedicated to model specific traffic situations, namely passing [24], jams [25] and flows [26], [27]. Many analog signals measured in clinical medicine can be marked as chaotic if treated using advanced signal processing algorithms; such as the brain activity [28], heart activity [29], EEG [30] and others.

Of course, chaotic oscillators can be intentionally built as a lumped electronic network by following circuit synthesis methods. One approach utilize concept known as the analog computer; useful cookbook is [31] where this design process is explained in step-by-step manner. Nice examples of analog chaotic oscillators implemented as the analog computers can be found in [32]–[34]. This method is straightforward, but drawback of designed circuitries is evident: huge number of active elements. Conventional circuit synthesis combines nonlinear passive device with active linear sub-circuit; check composites provided in [35]–[40]. Long time these kinds of realizations were supposed to be the simplest one; i.e. contain minimum number of the circuit components. Design process leading to fully integrated chaotic oscillators also belongs to the well-established knowledge, see [41]–[43]. Intentionally created electronic chaotic systems can be used as the core engines in various applications such as the random number generators [44], [45], chaos-based modulation [44], [46] and masking techniques [47], control systems [48], etc.

However, sometimes chaos represents unwanted operation regime of radio-frequency functional blocks. Quite logically chaos was noticed in RC feedback [49]–[51], Colpitts [52] and Hartley [53] oscillators. If we are speaking about driven systems high-Q active frequency filters with common KHN structure belong to the classical sources of chaotic signals [54]–[56]. Next, chaos as robust behavior has been detected in buck [57] and cuk [58] topologies or DC-DC converters in general [59]–[62], switching-mode power supplies [63], motor drives [64], switched capacitor networks [65] and regulators [66] can exhibit a random-like behavior under specific working conditions close to the common operation. Multi-stability and hidden attractors were localized within dynamics of relay system [67]. Unexpected chaotic response was reported in fundamental configuration of a phase-locked loop [68], [69] which is standard radio-frequency functional block. Traces of chaos were discovered in the logic gates [70] as well as in the different conceptions of the multiple-valued static memory cell; both with piecewise-linear [71] and polynomial [72] approximation of the resonant tunneling diodes. Here, we can find direct connection between number of the stable states and complexity of the chaotic attractors.

Existence of a robust chaos in a variety of algebraically non-conjugate third-order mathematical models launched a bit different research: find chaotic dynamics having equilibrium point-like, located on plane structure and three-dimensional. First class, i.e. systems with unstable fixed points, has been long time adopted as common standard for the chaotic flows. These equilibrium points were originally saddle-focuses but, as shown in [73], it is not mandatory. Also, the number of the fixed points is not restricted; chaotic flows with single unstable [74], single [75], [76], two [77], [78] stable fixed points were coined. In the context of these discoveries, it is not such a surprise that chaotic solutions can evolve in the vector fields where combination of stable and unstable fixed points creates its dynamics [79], [80]. A much bigger surprise is existence of chaos in dynamical system without equilibria [81]. Research studies involving the point-type equilibriums have been generalized to any number of the fixed points [82] including infinite many fixed points [83]. Equilibriums are all geometrical structures that satisfy a system of nonlinear algebraic equations $d\mathbf{x}/dt = 0$. Solution of this problem can degenerate to the higher-order (from the topological sense) geometrical structures but still preserving chaotic behavior. Gallery of the selected contributions to this kind of research can be briefly summarized as follows. Firstly, reader can recognize autonomous chaotic dynamical systems with line-type [84], [85], conic-shaped [86], circular [87] and square [88] equilibrium. Some papers were devoted to sum-up chaotic dynamics with the equilibrium structure of the same type, see [89] dealing with curve equilibrium, [90] bringing plane-type equilibrium and [91] where different equilibrium surfaces are discussed. Thus, chaotic dynamical system having variable equilibrium with parameter change [92] is nothing less but one logical step further. Despite many publications, research in this area is by no way closed.

After years of intensive searching for the algebraically simplest chaotic systems launched by H.P.W. Gottlieb J.C. Sprott seems to be the most successful scientist in this field. Few examples of the trivial continuous chaotic flows can be found in the papers of fundamental importance [93]–[97] or references given therein. The essence of chaos implies that probability of the chaotic solution, at least its existence for the specific sets of the initial conditions and values of the system parameters, raises with dimensionality of system. Because dynamical system describing real events is always nonlinear (at least if a general model close to the reality is considered) chaos still attracts increasing attention among

physicists, mathematicians and electrical engineers. Despite many years of a successive research focused on the lumped chaotic oscillators, the authors still believe that individual circuit structures proposed in the upcoming paper sections represent the simplest possible topologies suitable for both educational and technical application purposes.

This paper is organized as follows. Upcoming section introduces general concept utilized for fully analog chaotic oscillators based on the trans-resistance linear filters. Third part describes individual circuit realizations and provides computer-aided verification. Fourth section deals with numerical analysis closely bounded to the designed circuits. Fifth and sixth sections come with two modifications of the presented circuits: toward conservative chaotic oscillator [98] and inductor-free circuitry realizations. Finally, some concluding remarks are proposed in the seventh section.

II. DESCRIPTION OF SUB-CIRCUITS

Due to the fundamental properties of the chaotic signals each chaotic oscillator contains at least one energy source and one nonlinear element. Thus, with a view to achieving simplicity, it could be a good idea to combine both requirements and implement it as a single active two-port device [99], [100].

Assume a simple feedback connection of a general third-order low-pass filter and a nonlinear two-port as provided in Fig. 1. Suppose that third-order linear sub-circuit works in a trans-resistance operational mode while the nonlinear active two-port operates in a complementary trans-admittance regime. Such a situation can be described by the third-order ordinary differential equation. Here, we can distinguish between two situations. In the case of a trans-resistance filter with low-quality factor, namely if Q <1/2, we get

$$\frac{d^3}{dt^3}v_x - \frac{d^2}{dt^2}v_x \cdot \sum_{k=1}^{3}\omega_k - v_x \prod_{k=1}^{3}\omega_k + (\omega_1\cdot\omega_2 + \omega_1\cdot\omega_3 + \omega_2\cdot\omega_3)\frac{d}{dt}v_x = K_0 \cdot f\,(v_x)\cdot\prod_{k=1}^{3}\omega_k, \quad (1)$$

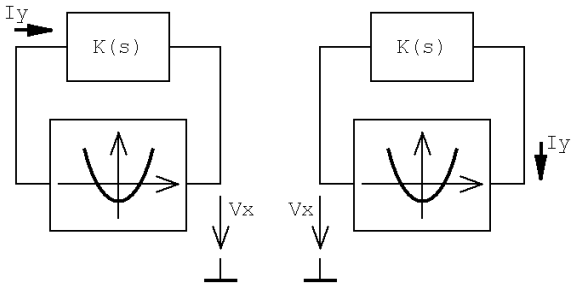

FIGURE 1. Fundamental concept of the proposed chaotic oscillators, with trans-impedance filter (left) and trans-admittance filter (right).

where ω_k is the angular frequency of k-th pole, K_0 is the transfer value of the filter in the pass-band and quantity v_x stands for the input voltage of nonlinear two-port element. For the filtering circuit having high-quality factor, namely if

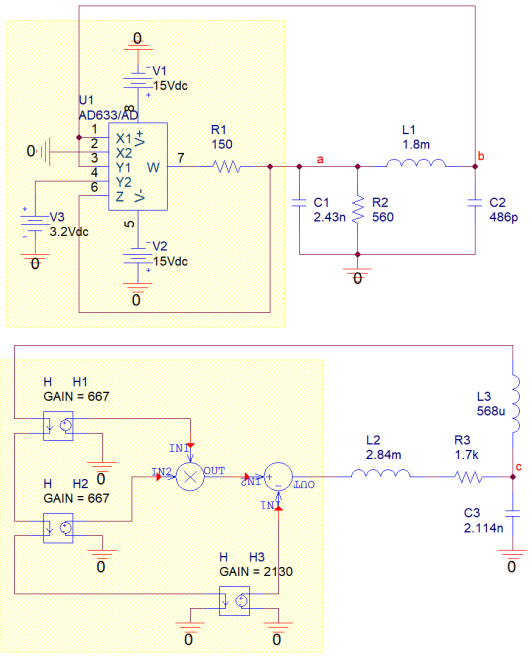

FIGURE 2. Circuit realizations of the flow-equivalent chaotic systems, with trans-impedance (upper) and trans-admittance (lower) two-port.

$Q > 1/2$, we obtain

$$\frac{d^3}{dt^3}v_x + \left(\frac{\omega_0}{Q} + \omega_p\right)\frac{d^2}{dt^2}v_x + \omega_0^2\cdot\omega_p\cdot v_x + \left(\omega_0^2 + \frac{\omega_0\cdot\omega_p}{Q}\right)\frac{d}{dt}v_x = \omega_0^2\cdot\omega_p\cdot K_0\cdot f\,(v_x), \quad (2)$$

where ω_0 is angular frequency of pair of complex conjugated poles, ω_p is angular frequency of real pole and $f(v_x)$ is scalar polynomial (quadratic) function. Note that both differential equations (1) and (2) represent the so-called jerk function that is known for its capability to exhibit strange attractors for many different choices of the nonlinear functions.

Of course, the low-pass immittance filters can be active. Such structures will not be members of the family of the canonical realizations (the simplest possible realization of a predefined mathematical model). On the other hand, all poles of trans-immittance function can be placed arbitrarily in the complex plane; i.e. all coefficients of the jerk function can have arbitrary values. Therefore, eigenvalues as the roots of a characteristic polynomial calculated at fixed points can be real or with the complex conjugated pair having positive or negative real parts. Thus, we can choose the stability index and local geometry near equilibrium points. Note that the maximal value of K_0 is unity for fully passive RC or RL realizations of the low-pass filtering section.

The proposed low-pass filtering concept and nonlinear feedback is, de facto, utilized in the fundamental memristor-based chaotic oscillator [101]. This circuit can be understood as a parallel connection of a biquadratic passive filter with admittance-type transfer function described by the Laplace

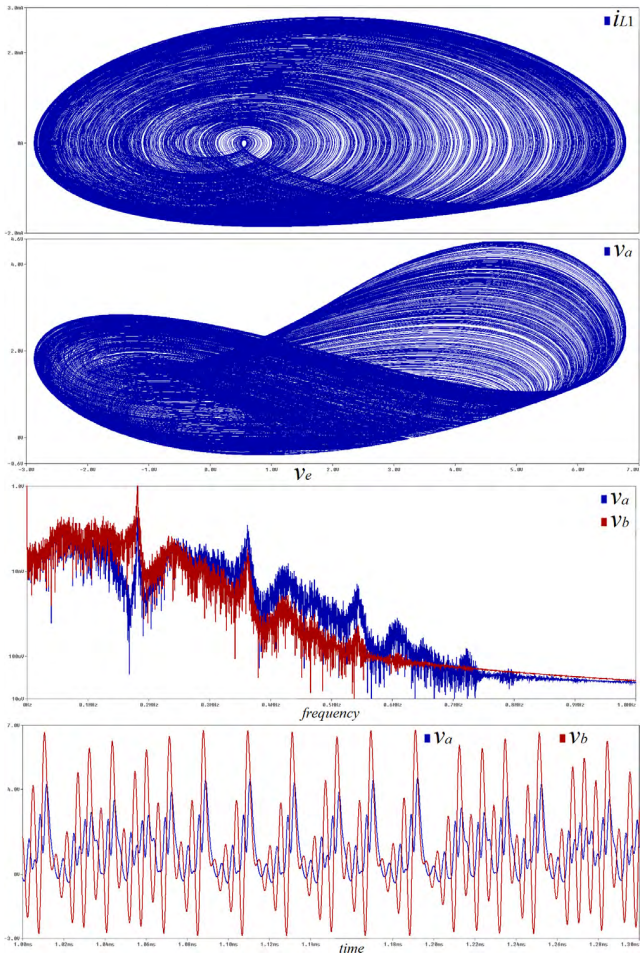

FIGURE 3. Orcad Pspice simulation: $i_{L1} - v_b$ and $v_a - v_b$ plane projection of the strange attractor (upper two plots), frequency spectrum of signal v_a (blue) and v_b (red), signal v_a (blue) and v_b (red) in the time-domain.

transform and single nonlinear memristive two-port element

$$K(s) = \frac{i_{in}(s)}{v_{in}(s)} = \frac{\omega_0^2 \cdot K_0}{s^2 + \omega_0 \cdot s/Q + \omega_0^2} \frac{d\, v_{in}}{d\, t} = f(i_{in}), \qquad (3)$$

where Q and ω_0 are the parameters of biquadratic circuit and s stands for complex frequency. Generally, memristors [102] as well as other mem-elements [103] are suitable components for design of analog chaotic oscillators because are described by promising pairs of the differential equations.

Although any kind of the nonlinear element can be used in design process of chaotic oscillator integrated circuit AD633 was finally chosen. Reason for this choice is versatile voltage transfer function of AD633, i.e. $V_W = K(V_{X1}-V_{X2})(V_{Y1}-V_{Y2})+V_Z$ where $K = 0.1$ is an internally trimmed constant. Such formula allows to create additional degree of freedom; possibility to adjust bifurcation parameter via external DC voltage to control chaos. All five input nodes of AD633 have a very large input resistance if compared to the working resistors. Thus, there are no leakage currents that can be expressed as error terms in the describing ordinary differential equations. Moreover, if it is connected properly,

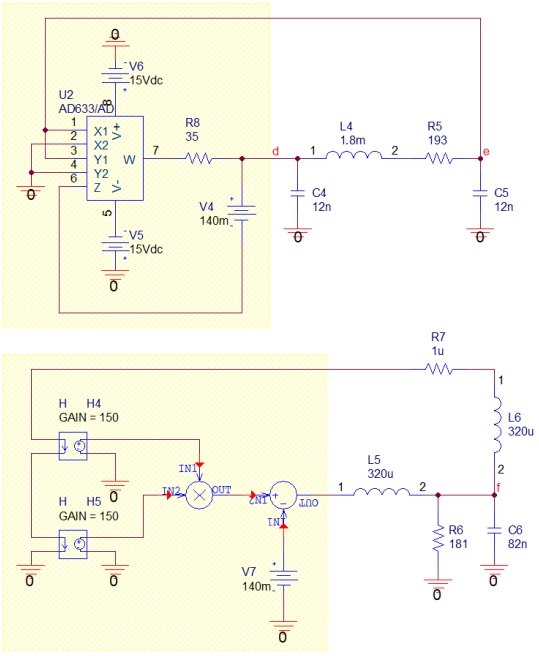

FIGURE 4. Circuit realizations of the flow-equivalent chaotic systems, with trans-impedance (upper) and trans-admittance (lower) two-port.

AD633 can work in different operational regimes as two-port voltage-to-voltage, two-port voltage-to-current or two-terminal, i.e. nonlinear resistor [104]. Suitable configuration can also compensate terms in the linear filtering two-port or make other benefits.

III. DESIGN EXAMPLES, CIRCUIT DESCRIPTION AND COMPUTER-AIDED VERIFICATION

Suppose two-port trans-resistance filter composed by two capacitors, one inductor and one resistor as demonstrated in Fig. 2 (upper schematic). Note that final chaotic system is very simple because contains single active and five passive elements. Its behavior is uniquely determined by following mathematical model

$$\begin{aligned} C_1 \frac{d\, v_a}{d\, t} &= -\frac{v_a}{R_2} - i_{L1} + \frac{K}{R_1}\left(v_b^2 - V_3 \cdot v_b\right) \\ C_2 \frac{d\, v_b}{d\, t} &= i_{L1} L_1 \frac{d\, i_{L1}}{d\, t} = v_a - v_b, \end{aligned} \qquad (4)$$

where the state vector is $x = (v_a, v_b, i_{L1})^{\mathrm{T}}$. Dynamical motion of this system is invariant under linear transformation of the coordinates $x \to -x$, $y \to -y$ and $z \to -z$. Described system can be expressed accordingly to the equation with the filter-type parameters (2), namely

$$\begin{aligned} \frac{d^3}{d\, t^3} v_b + \frac{1}{C_1 R_2} \cdot \frac{d^2}{d\, t^2} v_b + \frac{C_1 + C_2}{C_1 C_2 L_1} \cdot \frac{d}{d\, t} v_b \\ = \frac{v_b}{C_1 C_2 L_1}\left[\frac{K}{R_1}(v_b - V_3) - 1\right]. \end{aligned} \qquad (5)$$

Numerical optimization algorithm roughly discussed in [105] and [106] was utilized to find chaotic solution associated with

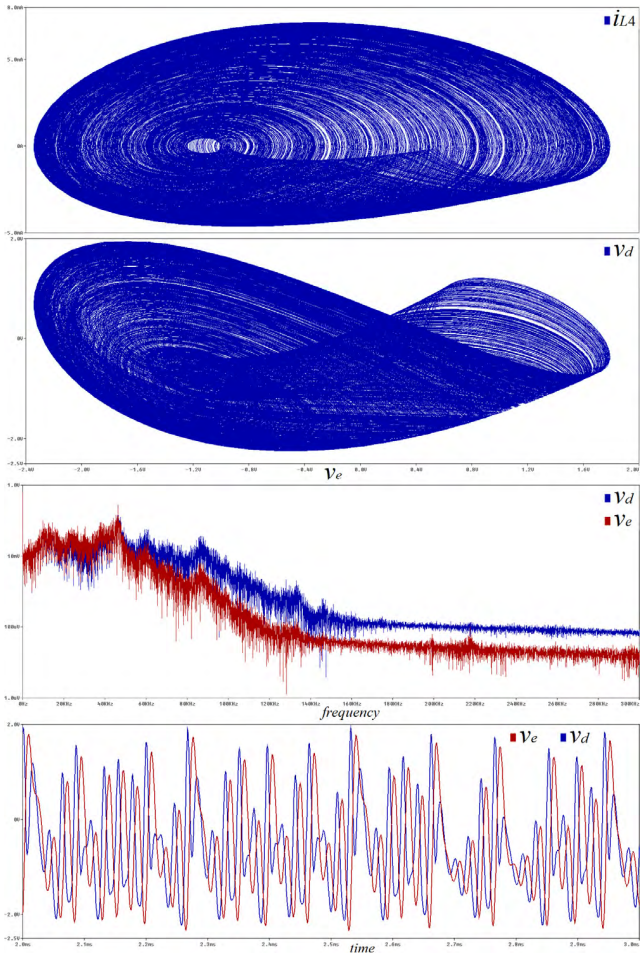

FIGURE 5. Orcad Pspice simulation: $i_{L4} - v_e$ and $v_d - v_e$ plane projection of the strange attractor (upper two plots), frequency spectrum of signal v_d (blue) and v_e (red), signal v_d (blue) and v_e (red) in the time-domain.

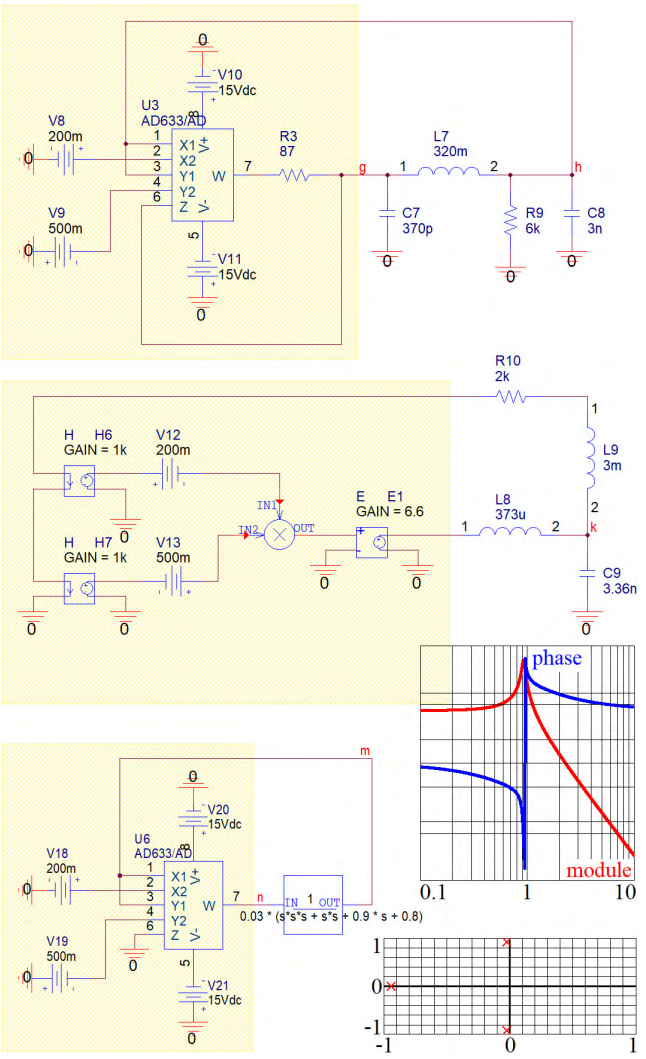

FIGURE 6. Circuit realizations of the flow-equivalent chaotic systems, with trans-impedance (upper picture), trans-admittance (middle image) and voltage-mode (lower schematic) filtering two-port block.

mathematical model (4). As starting guesses, numerical values of the circuit components were picked with respect to the overall system dissipation and existence of equilibrium with saddle-focus type of vector field geometry. Since gradient method cannot be used in this case, full five-dimensional grid (table of values) is computed. Assuming numerical values of elements $L_1 = 1.8 \cdot \xi$ mH, $C_1 = 2.43 \cdot \xi$nF, $C_2 = 486 \cdot \xi$pF, $R_1 = 150\ \Omega, R_2 = 560\Omega$ and $V_3 = 3.32$ V, we can notice evolution of strange attractor with the locally maximal largest Lyapunov exponent (LLE); details will be specified in the next paper section. The proposed chaotic circuit allows easy frequency rescaling via the real positive constant ξ. This number can be used to shift a broad-band frequency spectrum into the audio range, toward high frequencies or to fit the true (measured) value of inductor. With $\xi = 1$ the fundamental frequency components of the generated chaotic signals fall within the frequency range from DC up to 750 kHz. For this case, parameters of a third-order trans-resistance filter in the sense of formula (2) are $\omega_p = 6406$ krad/s, $\omega_0 = 1145$ krad/s and $Q = 12.144$. Of course, frequency limitations are given by the roll-off effect of AD633. Analyzed dynamical flow has two fixed points located in state space position $\mathbf{x}_{e1} = [V_3 + R_1/(R_2K), V_3 + R_1/(R_2K), 0]^{\mathrm{T}}$,$\mathbf{x}_{e2} = [0, 0, 0]^{\mathrm{T}}$. Both equilibrium points are unstable providing saddle-focus local vector field geometry. Eigenvalues associated with $\mathbf{x}_{e1}$ are $\lambda_{1,2} = (-7.445 \pm j13.93) \cdot 10^5$ and $\lambda_3 = 7.541 \cdot 10^5$ while $\mathbf{x}_{e2}$ repels state trajectory accordingly to eigenvalues $\lambda_{1,2} = (1.721 \pm \mathrm{j}13.09) \cdot 10^5$ and $\lambda_3 = -10.79 \cdot 10^5$.

Figure 2 also contains network that is dual to a designed chaotic oscillator; i.e. state vector becomes $\mathbf{x}= (i_{L2}, i_{L3}, v_c)^{\mathrm{T}}$. Describing mathematical model can be written as follows

$$\begin{aligned} L_2 \frac{d\, i_{L2}}{d\, t} &= -i_{L2} \cdot R_3 - v_c + h_1 \cdot h_2 \cdot i_{L2}^2 - h_3 \cdot i_{L2} \\ L_3 \frac{d\, i_{L3}}{d\, t} &= v_c C_3 \frac{d\, v_c}{d\, t} = i_{L2} - i_{L3}, \end{aligned} \tag{6}$$

where h_k stands for a trans-resistance of k-th ideal current-controlled voltage source. This kind of circuit realization is not suitable for immediate design because it requires two

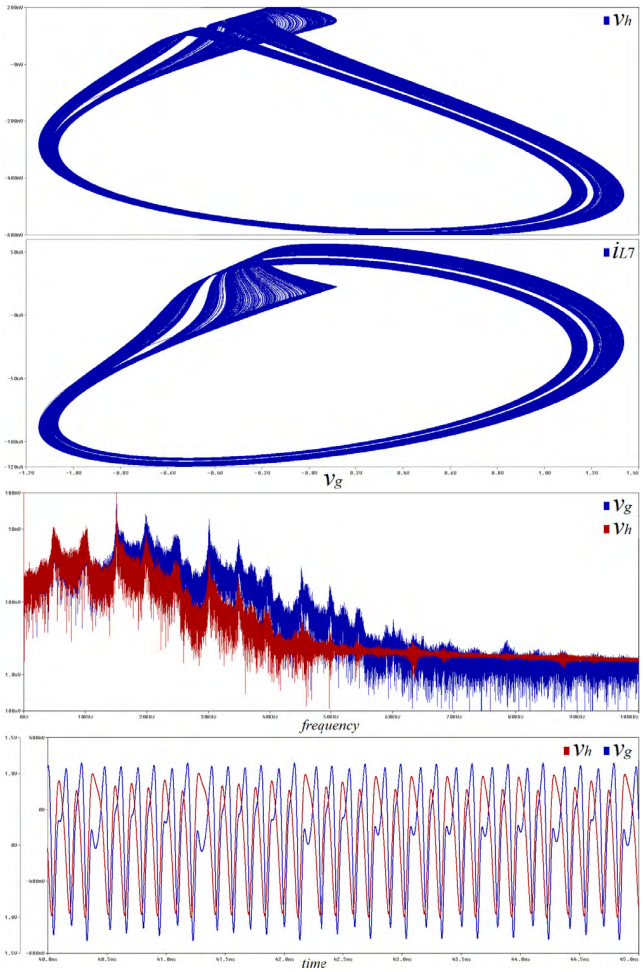

FIGURE 7. Orcad Pspice simulation: $i_{L7} - v_g$ and $v_h - v_g$ plane projection of the strange attractor (upper two plots), frequency spectrum of signal v_g (blue) and v_h (red), signal v_g (blue) and v_h (red) in the time-domain.

floating inductors and several hypothetic active elements. Nonlinear two-port (yellow section in Fig. 2) also contains a block for voltage multiplication (MULT) and difference of signals (DIFF). Circuitry implementations ready for Orcad Pspice simulation are provided in Fig. 2 while the achieved results can be judged by means of Fig. 3.

The second example of a chaotic oscillator consists of a trans-resistance filter, similar to the previous one, and active two-port where the output current is nonlinearly (quadratic polynomial) controlled by the input voltage. For details see Fig. 4 where dual circuitry implementation is demonstrated as well. In this case, state vector changes into $\mathbf{x}=\ (v_d,\ v_e,\ i_{L4})^{\mathrm{T}}$. The mentioned concept can be mathematically described by a set of the following ordinary differential equations

$$\begin{aligned} C_4\frac{d\,v_d}{d\,t} &= -i_{L4}+\frac{K}{R_4}v_e^2-\frac{V_4}{R_4}\\ C_5\frac{d\,v_e}{d\,t} &= i_{L4}L_4\frac{d\,i_{L4}}{d\,t}=v_d-v_e-R_5\cdot i_{L4}, \end{aligned} \tag{7}$$

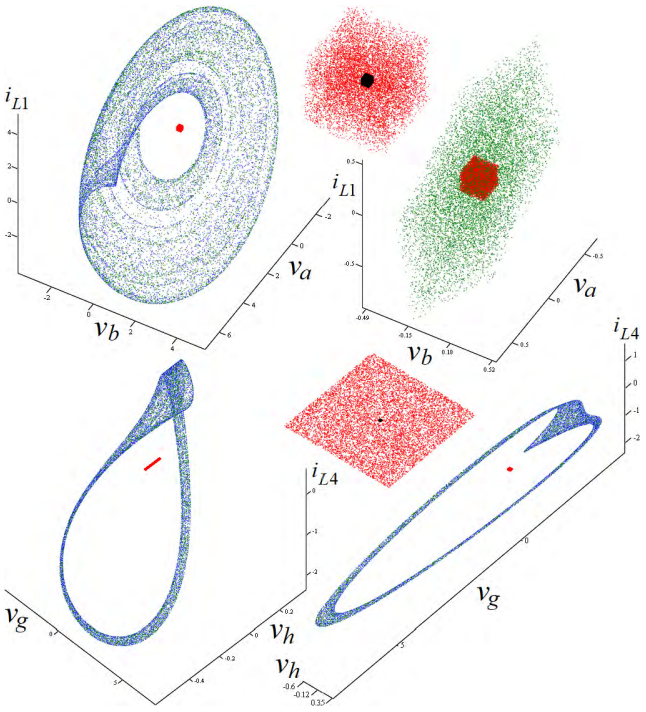

FIGURE 8. Numerical calculations and graphical visualization of time-domain sensitivities associated with dynamical system (4) (upper plots) and system (10) (lower plots), magnified cubes and planes showing uniform distribution of the initial conditions, see text for details.

which can be expressed in the filter-like fashion

$$\begin{aligned} &\frac{d^3}{d\,t^3}v_e+\frac{R_5}{L_4}\cdot\frac{d^2}{d\,t^2}v_e+\frac{C_4+C_5}{C_4C_5L_4}\cdot\frac{d}{d\,t}v_e\\ &\qquad=\frac{1}{C_4C_5L_4R_4}\left(K\cdot v_e^2-V_4\right). \end{aligned} \tag{8}$$

To observe robust strange attractor, network components can be fixed on the numerical values L_4 =1.8·ξ mH, $C_4 = 12.7\cdot\xi$nF, $C_5 = 12.7\cdot\xi$nF, $R_4 = 35\ \Omega$, $R_5 = 193\ \Omega$ and voltage V_4 =140 mV. Real-valued constant ξ can be used to convert the frequency components of the generated chaotic waveforms into more convenient frequency band. Orcad Pspice aided simulation results are provided in Fig. 5. Dual circuit with the state vector $\mathbf{x}=\ (i_{L5},\ i_{L6},\ v_f)^{\mathrm{T}}$ is described by following expression

$$\begin{aligned} L_5\frac{d\,i_{L5}}{d\,t} &= -v_f+h_4\cdot h_5\cdot i_{L6}^2-V_7\\ L_6\frac{d\,i_{L6}}{d\,t} &= v_f-R_7\cdot i_{L6}C_6\frac{d\,v_f}{d\,t}=i_{L5}-i_{L6}-\frac{v_f}{R_6}. \end{aligned} \tag{9}$$

Nonlinear trans-admittance type sub-circuit (see yellow region in Fig. 4) is created using MULT and DIFF functional blocks. Linear part of the vector field (trans-impedance two-port) of this dynamical system has a single zero pole and pair of complex conjugated leading to quality factor Q =2.759 and pole frequency ω_p =296 krad/s. Once again, frequency limits are defined by the parasitic filtering effect of AD633 device. Dynamical system (7) contains a pair of

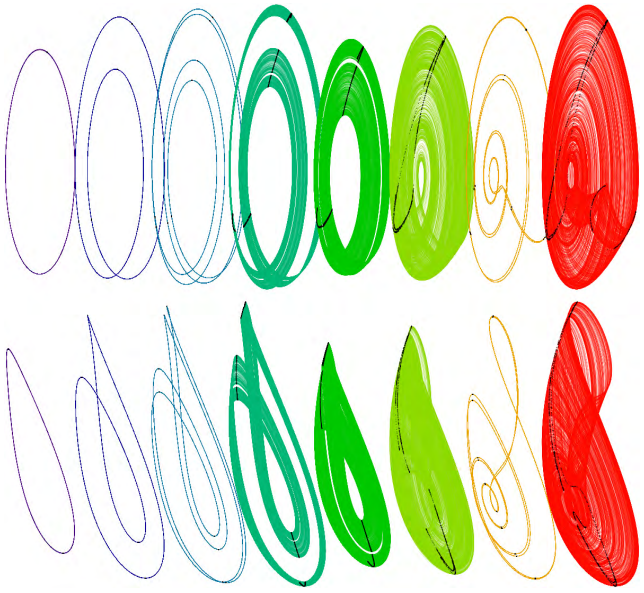

FIGURE 9. Bifurcation scenario visualized as plane projection v_d vs i_{L4} (upper row) and $v_d - v_e$ with respect to the external voltage V_4 (see text).

the fixed points, namely $\mathbf{x}_{e1} = (\sqrt{V_4/R_4}, \sqrt{V_4/R_4}, 0)^{\mathrm{T}}$,$\mathbf{x}_{e2} = (-\sqrt{V_4/R_4}, -\sqrt{V_4/R_4}, 0)^{\mathrm{T}}$. Both points represent unstable equilibrium having saddle-focus local vector field geometry. Eigenvalues associated with $\mathbf{x}_{e1}$ are $\lambda_{1,2} = (-1.396 \pm \mathrm{j}3.406) \cdot 10^5$ and $\lambda_3 = 1.719 \cdot 10^5$ while fixed point $\mathbf{x}_{e2}$ spirals away state trajectory accordingly to the eigenvalues $\lambda_{1,2} = (0.525 \pm j3.271) \cdot 10^5$ and $\lambda_3 = -2.122 \cdot 10^5$.

Finally, the third example of a canonical chaotic oscillator (see Fig. 6), can be described by the mathematical model

$$\begin{aligned} C_7 \frac{d\, v_g}{d\, t} &= -i_{L7} + \frac{K}{R_3}\,(v_h - V_8) \cdot (v_h + V_9) \\ C_8 \frac{d\, v_h}{d\, t} &= i_{L7} - \frac{v_h}{R_9} L_7 \frac{d\, i_{L7}}{d\, t} = v_g - v_h, \end{aligned} \tag{10}$$

where the state vector is $\mathbf{x}$= $(v_g, v_h, i_{L7})^{\mathrm{T}}$. Dynamical motion of this circuit can be described by single third-order differential equation, i.e. formula directly comparable to (2), namely

$$\begin{aligned} &\frac{d^3}{d\, t^3} v_h + \frac{1}{C_8 R_9} \cdot \frac{d^2}{d\, t^2} v_h + \frac{C_7 + C_8}{C_7 C_8 L_7} \cdot \frac{d}{d\, t} v_h \\ &\quad + \frac{1}{C_7 C_8 L_7 R_9} v_h = \frac{K}{C_7 C_8 L_7 R_3}\,(v_h - V_8) \cdot (v_h + V_9)\,. \end{aligned} \tag{11}$$

Typical strange attractor can be generated by this network for the following numerical values of the circuit components L_7 =320·ξ mH, C_7 =370·ξpF, C_8 =3·ξnF, R_3 =87 Ω, R_9 =6 kΩ and voltages V_8 =200 mV, V_9 =500 mV; ξ being real constant. Chaotic oscillator that is dual to discussed topology is given in Fig. 6 with two-port nonlinearity marked by yellow color. Covering set of the ordinary differential equations is

$$L_8 \frac{d\, i_{L8}}{d\, t} = -v_k + e_1\,(h_6 \cdot i_{L9} - V_{12}) \cdot (h_7 \cdot i_{L9} + V_{13})$$

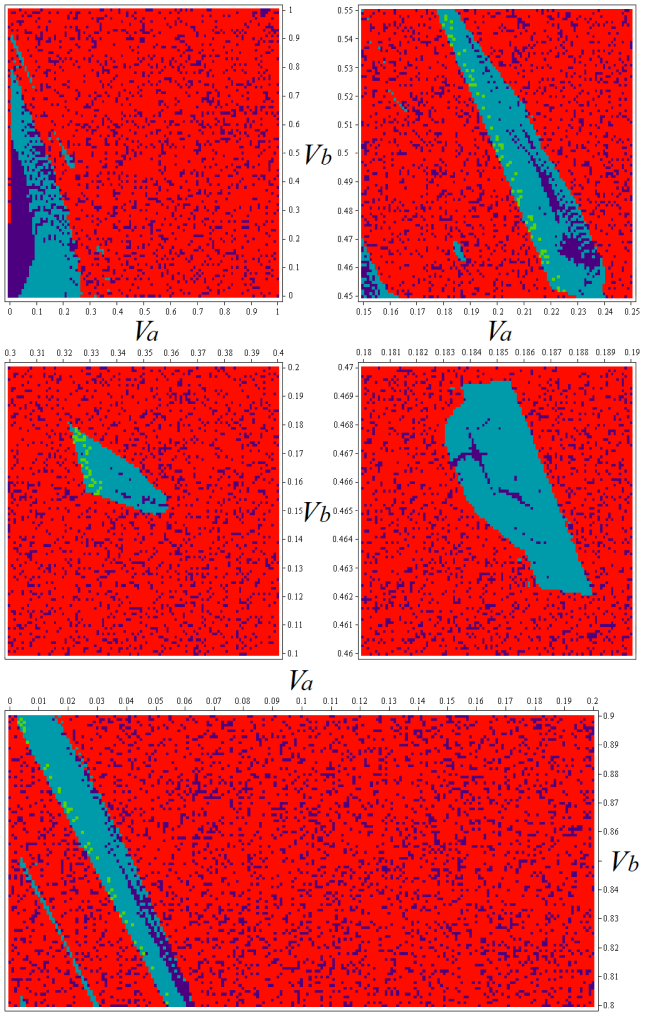

FIGURE 10. Different solutions of dynamical system (10) with respect to values of the external DC voltages V_8 and V_9: fixed point (dark blue), limit cycle (light blue), chaos (green) and unbounded solution (red).

$$L_9 \frac{d\, i_{L9}}{d\, t} = v_k - R_{10} \cdot i_{L9} C_9 \frac{d\, v_k}{d\, t} = i_{L8} - i_{L9}, \tag{12}$$

where e_1 is the gain of an ideal voltage-controlled voltage-source, blocks h_6 and h_7 convert input current of nonlinear two-port to pair of voltages. In practice, this operation could be done by the so-called Norton amplifiers. Few types are currently commercially available now; for example, LM3900 or LM359. However, final circuit complexity is significantly raised and state vector changes into $\mathbf{x}$= $(i_{L8}, i_{L9}, v_k)^{\mathrm{T}}$. We can also replace concept of immittance filter by common voltage-mode filter, see chaotic oscillator in Fig. 6. This structure can be either passive or active; its transfer properties are defined by block LAPLACE. Note that this oscillator is normalized with respect to time. Real filter parameters can be obtained after substitution $\tau \cdot \mathrm{s} \rightarrow \mathrm{s}$ where τ is time constant in seconds. Module (60 dB down to -40dB) and phase (scale 200° down to -200°) frequency response of the black-box filter as well as locations of transfer poles are provided via

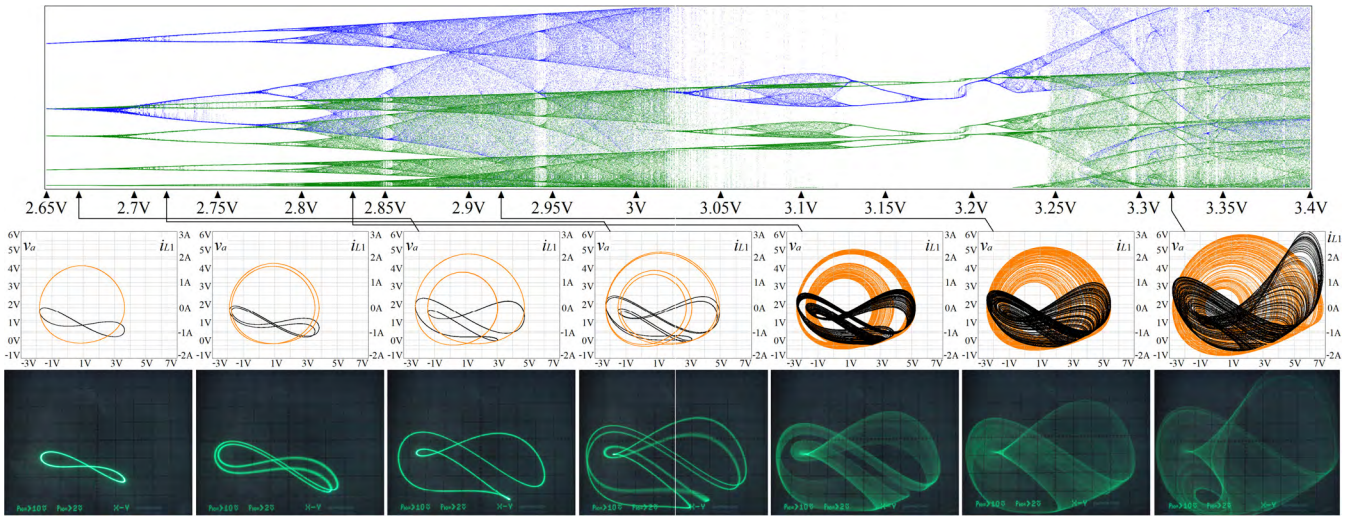

FIGURE 11. High-resolution bifurcation diagram calculated with respect to the external voltage V_3, numerical integration process vs experimental measurement for (from the left to right): V_3 =2.3 V, V_3 =2.36 V, V_3 =2.3 V, V_3 =2.67 V, V_3 =2.72 V, V_3 =2.92 V and V_3 =3.32 V, plane projection v_1 vs v_2 (black curve) and i_{L1} vs v_2 (orange trajectory), corresponding v_1 vs v_2 Monge projections captured by oscilloscope.

Fig. 6. Note that poles have negative real part; i.e. filter operates in stable area.

Existence and number of the fixed points depends on the values of the external voltages V_8 and V_9. The location of equilibrium can be expressed as $\mathbf{x}_e = (v_x, v_x, v_x/R_9)^{\mathrm{T}}$, where v_x are the real solutions for voltage of the quadratic polynomial $v_x^2 + v_x[V_9\text{-}V_8\text{-}R_3/(R_9K)]\text{-}V_8V_9 = 0$. Therefore, the equilibrium points exist only under fulfilling $[V_9\text{-}V_8\text{-}R_3/(R_9K)]^2 > 4 \cdot V_8 \cdot V_9$. For numerical values of the circuit parameters provided above we get a pair of the fixed points; the first one is in position $\mathbf{x}_{e1} = (-0.403, -0.403, -67.2 \cdot 10^{-6})^{\mathrm{T}}$ while the second one is located at $\mathbf{x}_{e2} = (0.248, 0.248, 41.3 \cdot 10^{-6})^{\mathrm{T}}$. Simulation results obtained by using Orcad Pspice are depicted in Fig. 7.

IV. NUMERICAL ANALYSIS OF CHAOTIC CIRCUITS, EXPERIMENTAL MEASUREMENT

Since the main topic of this paper is a presentation of new chaotic oscillators all results coming from numerical analysis are directly bounded to designed electronic system and local circuit parameters. Numerical integration processes were performed in Mathcad using build-in fourth-order Runge-Kutta method with fixed step size. The same program was utilized for graphical visualization of all results. Program MATLAB was adopted for LLE routine where *ode45* solver and Gram-Smith orthogonalization have been used.

As already mentioned, behavior of the chaotic systems is sensitive to the changes of the initial conditions. This fact is proved by means of Fig. 8 where many state trajectories (10^4) with negligible initial separation (in the vicinity of zero) were numerically integrated and final states were visualized. In the case of first chaotic system (upper plots), initial conditions were randomly generated inside the cube with side length 0.1 (red dots) and 0.01 (black dots). Left graph shows long-term evolution with final $t_{max} = 100$ s (green points) while right plot offers short-time separation after $t_{max} = 10$ s (blue final states). Lower plots demonstrate extreme sensitivity to the initial conditions of dynamical system (10). However, because of thin basins of attraction in z-dimension, initial conditions are randomly swept over the plane $z = 0$, with side size 0.05 (red points) and 0.001 (black points). Both plots show a long-term evolution with final time $t_{max} = 1000$ but for the differently rotated state space. Deep numerical investigations show that system (10) has higher level of predictability than system (4).

Typical route-to-chaos scenario in the second discovered chaotic system (7) is shown by means of Fig. 9. It represents numerically integrated period-doubling bifurcation scenario plotted using rainbow color scale. This sequence is provided with respect to the change of the external DC voltage V_4; numerical values and corresponding state attractors from left to right: 76 mV, 88 mV, 92 mV, 94 mV, 96 mV, 100 mV, 105 mV and 112 mV. Note that small variation of this external parameter can burn or bury desired strange attractor. Cross section for visualization of Poincare return maps (black dots) is a plane defined by zero current through the inductor. Increasing voltage above value 112 mV leads to a dynamical solution which is unbounded for almost all configurations of the initial conditions.

The concept of LLE, that is calculation of LLE with respect to some circuit parameters, was used for a dynamical flow quantification associated with the third proposed chaotic system. Since both voltages V_8 and V_9 can seriously affect parameters of the linear filter, namely value of product $\omega_0^2\omega_p$, precise combination of these voltages should be achieved and kept precisely during experimental verification. This is documented by means of Fig. 10 where four different types

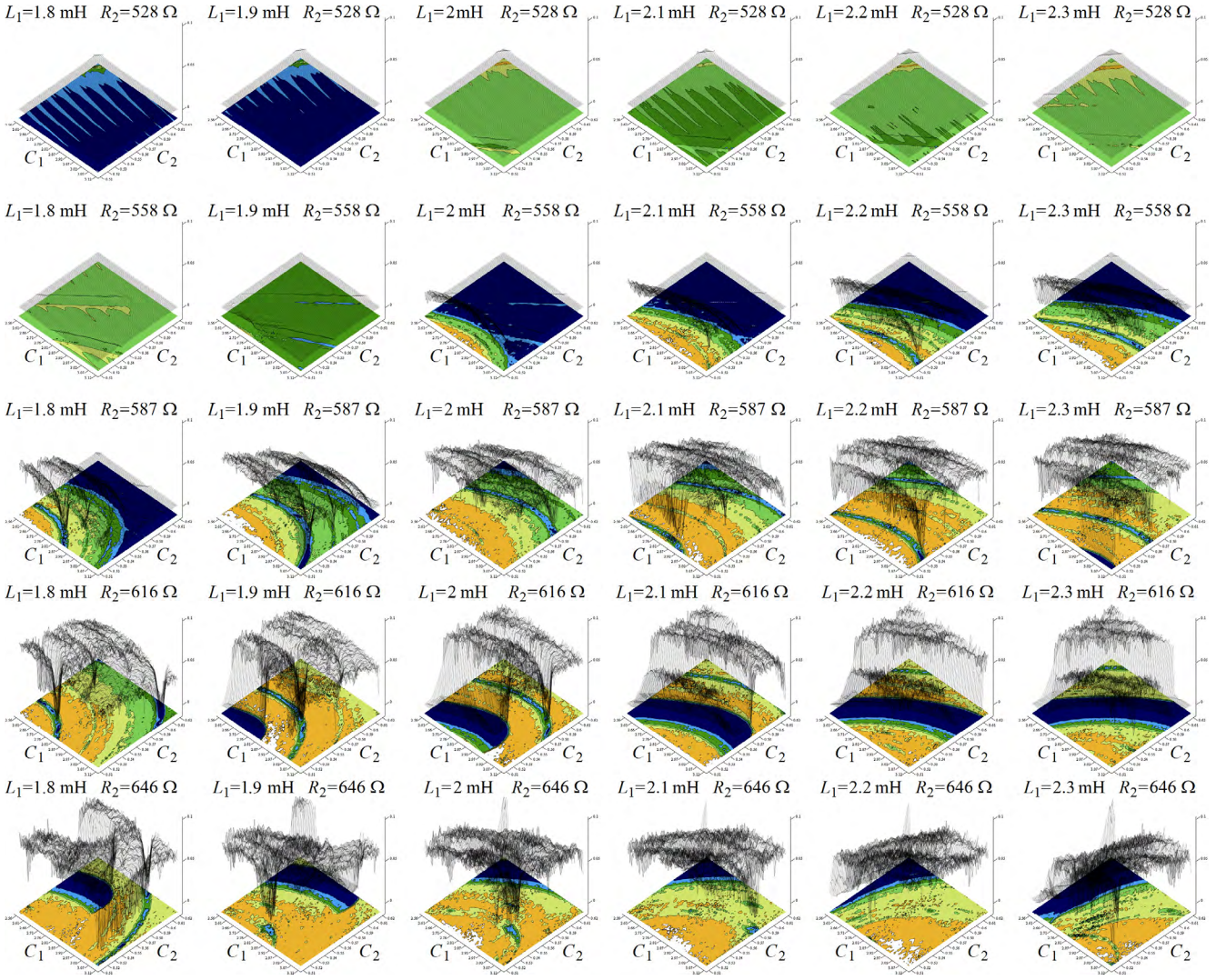

FIGURE 12. Topographically-scaled surface-contour plots of LLE calculated in a 4D cube of circuit parameters and for external DC voltage V_b =2.9 V: horizontal axis represents six different numerical values of floating inductor while vertical axis shows five different numerical values of resistor R_1. Color scale: fixed points (blue), limit cycles (green), chaos (yellow) and unbounded solution (white).

of solution visualized in the two-dimensional plane $V_8 \in (0, 1)$ and $V_9 \in (0, 1)$ are given. Here, voltage step 0.01 for basic (upper plot) and 0.0001 (middle right plot) and 0.001 (all other images) for zoomed sub-planes are provided. This calculation was performed for sets of initial conditions taken from close neighborhood of zero. Note that only a few combinations of the voltages result into steady state strange attractor. Investigated parameter space is filled by unbounded solution, i.e. a state trajectory exhibits chaotic transient and quickly escapes to infinity. Extreme sensitivity of behavior to voltages can find its place in the sensor applications.

One-dimensional bifurcation diagram associated with the dynamical system (4) and calculated with respect to external voltage V_3 is provided by means of Fig. 11. Each colored slice represents a plane given as z-1, state variable x (blue) and y (green), final integration time 10^4 with time step 10^{-3} and voltage step 0.0001. This graph is completed by showing theoretically expected shapes of strange attractors, obtained using the normalized mathematical model of a chaotic oscillator, as well as practically measured Monge-projections of the same attractors using oscilloscope. Note that chaotic operation of designed oscillator alternates with windows, where this circuit exhibits variety of the periodic solutions. Standard period-doubling route to chaos scenario has been confirmed both by numerical analysis and practical survey.

The robustness of the strange attractors, i.e. structural vulnerability against tolerances of the network components, is a well-established measure that commonly defines practical applicability of the continuous-time chaotic system. Since values of circuit elements are not analytically (that is by closed-form formula) coupled with the existence of chaos (this holds for both weak and strong chaos) some precise, trustworthy and easy-to-be-calculated dynamical flow-quantifier needs to be adopted. Sensitivities expressed

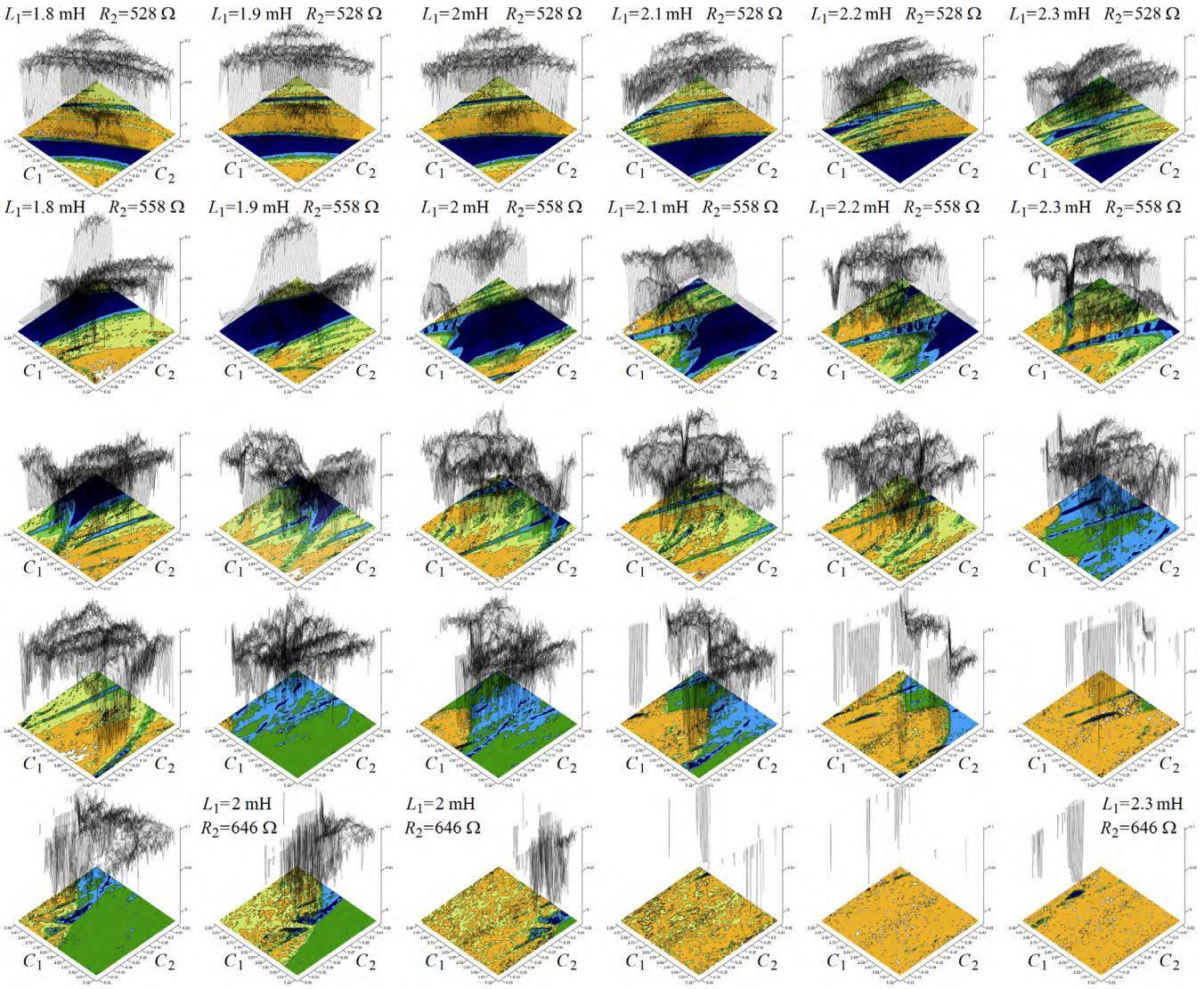

FIGURE 13. Topographically-scaled surface-contour plots of LLE calculated in a 4D cube of circuit parameters and for external DC voltage V_b =3.32 V: horizontal axis represents six different numerical values of floating inductor while vertical axis shows five different numerical values of resistor R_1. Color scale: fixed points (blue), limit cycles (green), chaos (yellow) and unbounded solution (white).

in the terms of LLE have been established and provided in topographically-scaled colored fashion in Fig. 12 and Fig. 13 for two different external voltages. These represent high-resolution plots having total number $101 \cdot 101 = 10201$ points. Obviously, area with a positive LLE is not centered and, as consequence, numerical values of the oscillator components can be updated to reach higher structural stability. However, in the actual situation, this area is wide enough such that the anticipated geometry of the strange attractor is structurally stable and easily experimentally observable even for real circuit components with tolerances and time fluctuations.

Calculation of basins of attraction for individual chaotic systems is another useful kind of the numerical investigation, important especially from the viewpoint of upcoming circuit realization. Based on the achieved results, it seems that there is no need to impose initial conditions to nodes (voltages) or branches (currents) of designed chaotic oscillators. However, in general, narrow basins not including surroundings of zero, leading to evolution of desired strange attractor, can represent serious problems in the case of practical experiments.

V. CONSERVATIVE CASES OF CHAOTIC CIRCUITS

Proposed topologies of the chaotic oscillators can be easily modified to exhibit the so-called conservative dynamics; that is volume-conserving strange attractor. Principal differences between robust dissipative and conservative dynamics can be understood by using appropriate visualization of state space, see Fig. 15. Here, both static and dynamic energy profiles are put into the context of time. These quantities are defined for time instances $k \in (0, 200)$ as measure $E_{static}(k) = \sqrt{[x_k^2 + y_k^2 + z_k^2]}$ and $E_{dynamic}(k) = \sqrt{[(x_k - x_{k-1})^2 + (y_k - y_{k-1})^2 + (z_k - z_{k-1})^2]}$ respectively. Maximal energy levels are marked by numerical values.

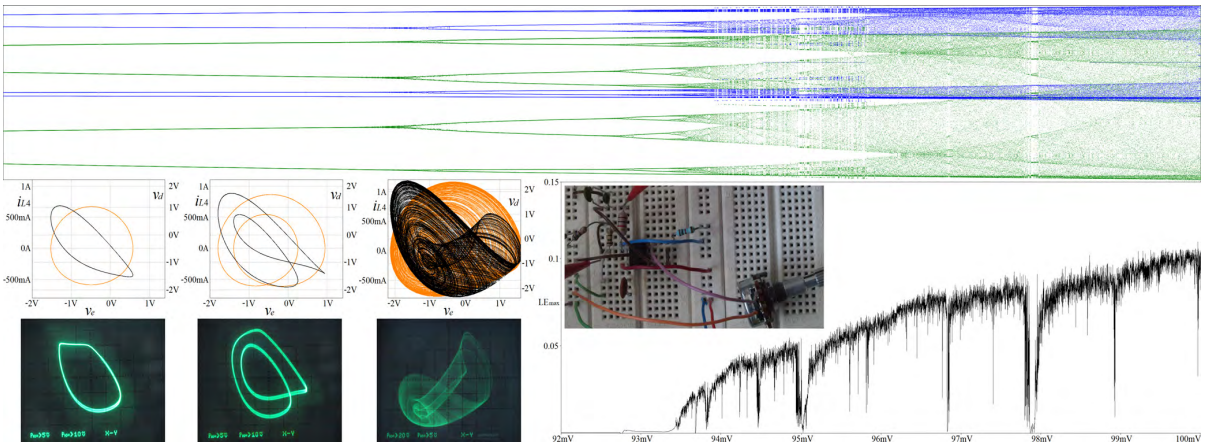

FIGURE 14. One-dimensional bifurcation diagram with respect to the external DC voltage V_4 in the range from 85 mV to 100 mV, corresponding graph of LLE focused on the range 92 mV to 100 mV, photograph of the bread-board with chaotic oscillator during measurement, selected plane projections of period-one, period-two and chaotic motion of constructed circuit ready for comparison between theoretical expectations and real observations.

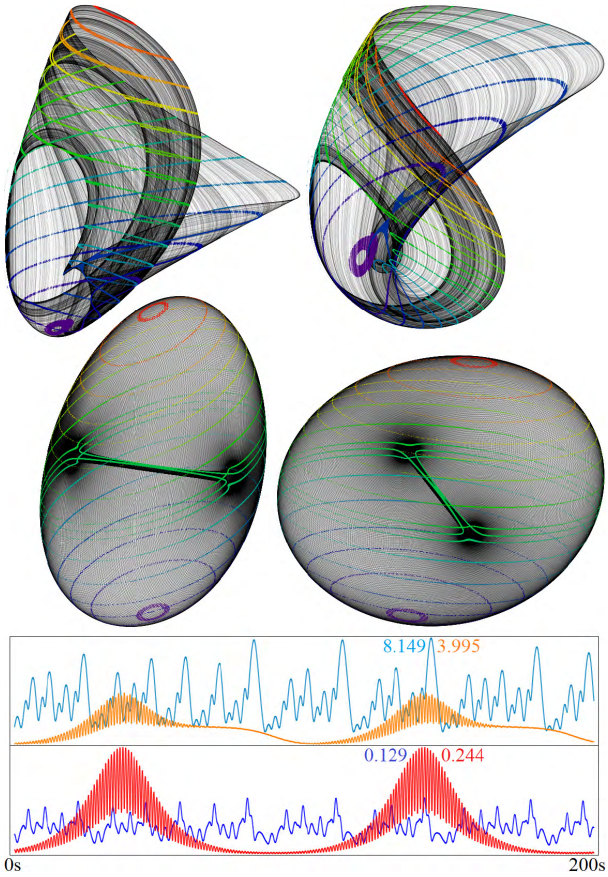

FIGURE 15. Rainbow-scaled (in z-axis direction) Poincaré sections of dissipative (upper two plots) and conservative (lower pair of images) typical strange attractors, static energy distribution of dissipative (light blue) and conservative (orange) system vs time, dynamic energy distribution of dissipative (light blue) and conservative (orange) system.

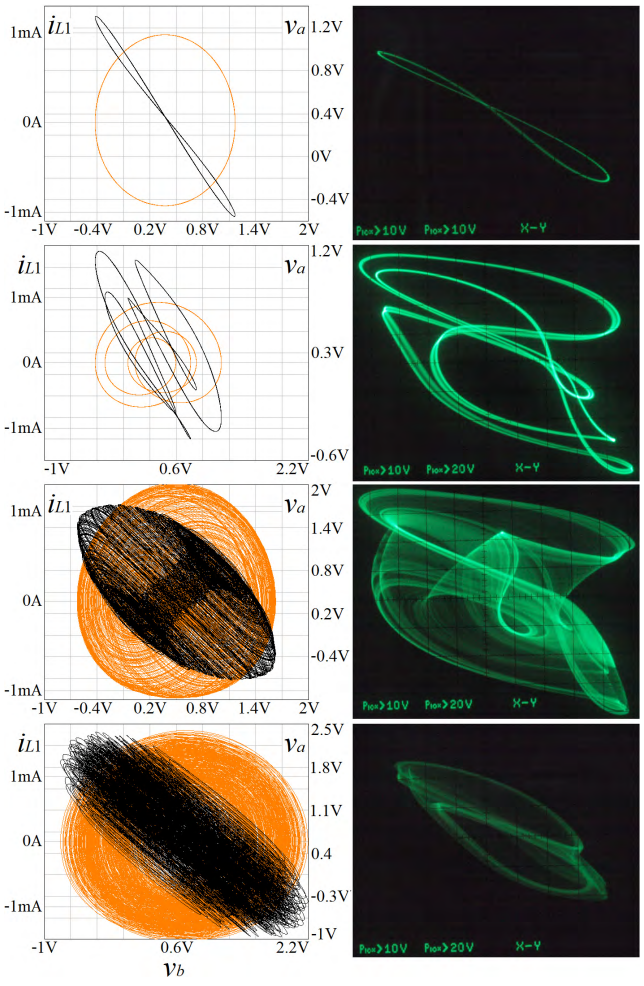

FIGURE 16. Comparison between numerically calculated (left column) and experimentally observed (right column) state attractors observed within dynamics of conservative system.

Note that by considering resistor R_2 removed dynamical system (4) turns to be conservative [107], [108]; that is with the volume preserving state attractor. Thus, one example of conservative chaos can be modeled by the network shown in Fig. 2 (upper schematic) by considering choice $R_2 \rightarrow \infty, L = 1.8$ mH, $C_1 = 1$ nF, $C_2 = 1.2$ nF and $R_1 = 220\ \Omega$. By variation of the external voltage V_3 from 900 mV

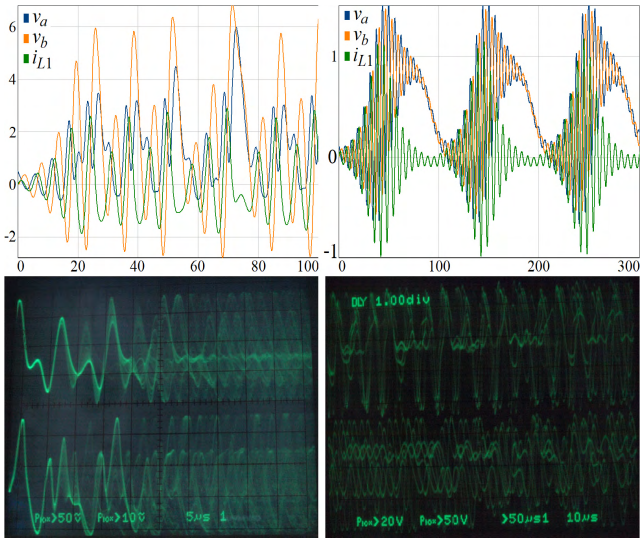

FIGURE 17. Brief comparison between waveforms in the time-domain: numerically integrated mathematical model having normalized time and impedances of dissipative (upper left plot) and volume-conserving (upper right plot) dynamics, measured waveforms generated by designed dissipative (lower left) vs conservative (lower right) chaotic oscillator and visualized in the time domain using oscilloscope.

up to approximately 1.1 V we can observe different state attractors; beginning with periodic and resulting into dense strange attractor. Boosting this voltage further leads to the unbounded behavior where AD633 saturates and do not work properly. Corresponding plane projection is singular point in position given by supply voltages. Measured plane projections are captured in Fig. 16 together with the state trajectories obtained by numerical integration process considering mathematical model with the real-valued circuit parameters. Note that there are differences caused by dissipation introduced into the chaotic oscillator by parasitic properties of the active element and common cheap inductor. Waveforms in time generated by both dissipative and conservative chaotic systems are shown in Fig. 17. Importance of practical experiments with chaos, except of proof of the structural stability, is that analog circuitry allows smooth change of the individual system parameters. This feature can cause that some interesting attractors are revealed during experimental measurement but not in the process of numerical analysis, see few examples provided in Fig. 18.

VI. INDUCTOR-LESS TOPOLOGIES OF CANONICAL CHAOTIC OSCILLATORS

From the viewpoint of experimental-oriented design the most promising structures of chaotic oscillators will be composed by resistors, capacitors and single nonlinear active device. This nonlinear circuit element can be piecewise-linear [109] as well as polynomial [110], connected as two-terminal or two-port. Since filtering network based on RC elements exhibits very low intrinsic quality factor this concept can

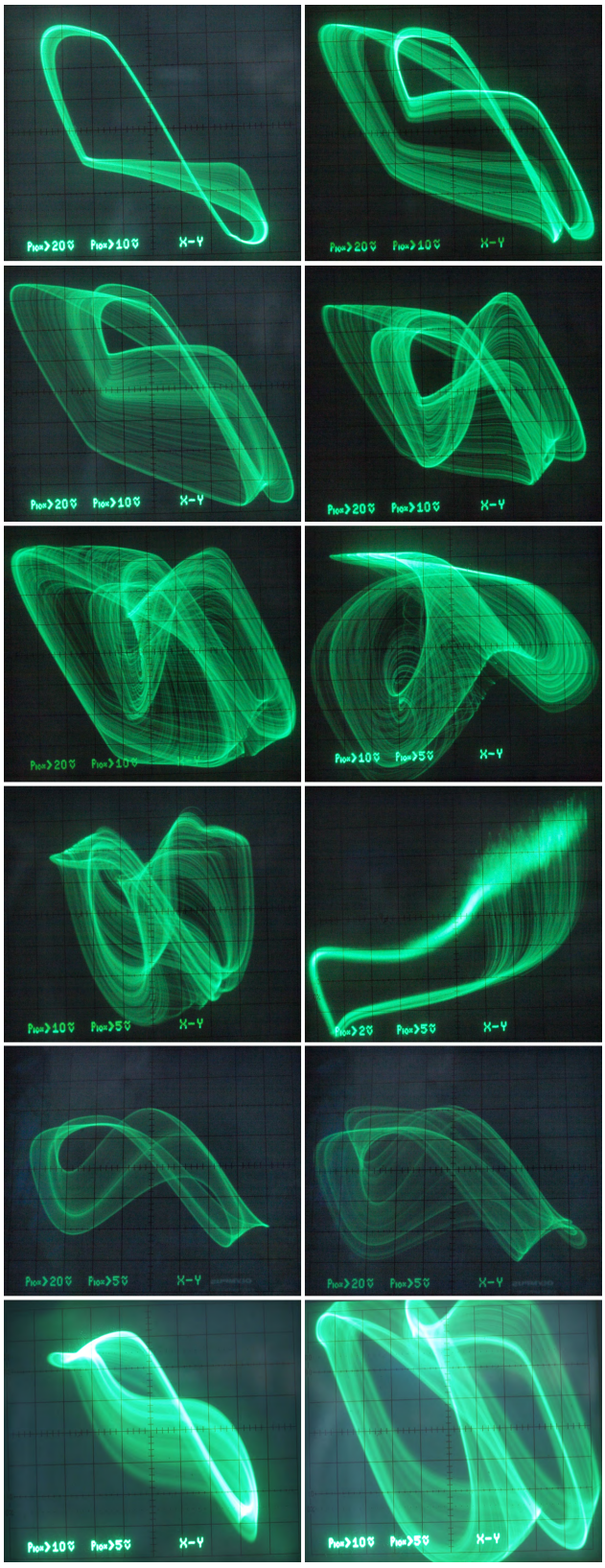

FIGURE 18. Interesting geometrical structures of the state attractors captured on oscilloscope during experimental measurement but not localized within numerical analysis of the differential equations.

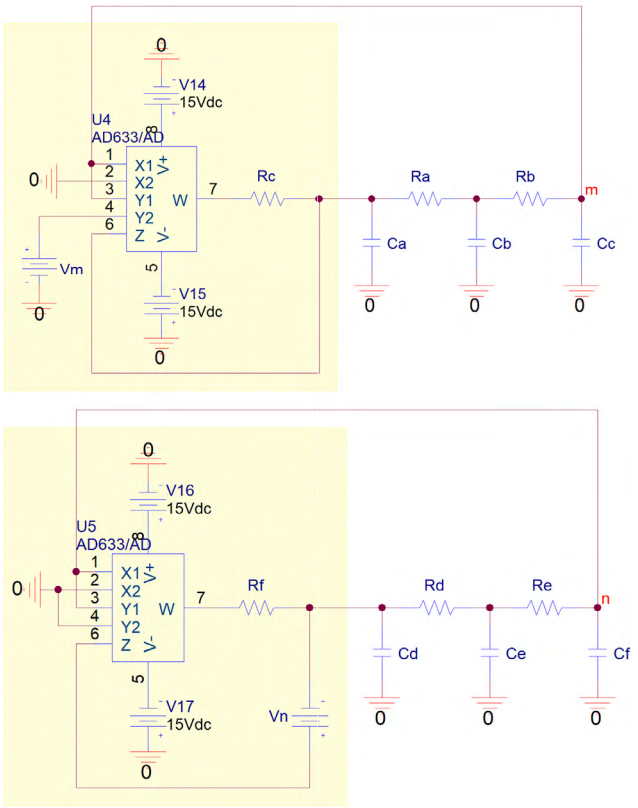

FIGURE 19. Potentially chaotic fully analog oscillators with lumped parameters based on the passive RC ladder network and simple polynomial active feedback of the trans-impedance type.

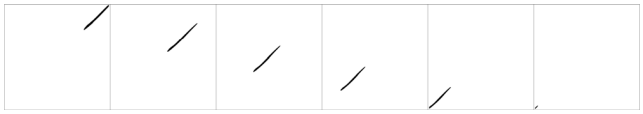

FIGURE 20. Basin of attraction (black dots) toward global chaotic attractor established for conservative dynamical system, see text.

be used for synthesis of dynamical systems with significant dissipation or in cooperation with nonlinear element having advantageous transfer function. Thus, this section will introduce several lumped networks that can be potentially chaotic. However, numerical values of the circuit elements need to be discovered using some optimization algorithm based on the describing mathematical model [111] or generated time sequence [112]. In the case of tabularized calculations parallel processing is highly recommended.

Let's consider first circuitry implementation provided in Fig. 19. This oscillator can be described by the following third-order ordinary differential equation

$$\frac{d^3}{dt^3}v_m + \left(\frac{R_a+R_b}{C_bR_aR_b} + \frac{1}{C_cR_b} + \frac{1}{C_aR_a}\right)\cdot\frac{d^2}{dt^2}v_m + \frac{C_a+C_b+C_c}{C_aC_bC_cR_aR_b}\cdot\frac{d}{dt}v_m = \frac{K\cdot v_m\,(v_m - V_m)}{C_aC_bC_cR_aR_bR_c}, \quad (13)$$

and represents alternative to dynamical system (4). By a slight modification of the network, second schematic in Fig. 19,

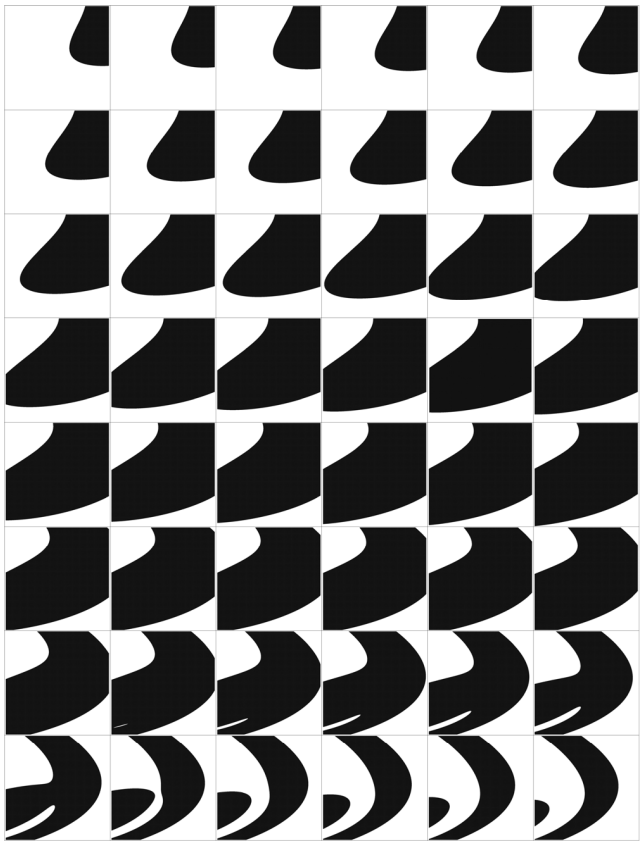

FIGURE 21. Basin of attraction (black area) toward global chaotic attractor calculated for dissipative dynamical system, see text.

we can obtain dynamics closely related to (7), namely

$$\frac{d^3}{dt^3}v_n + \left(\frac{R_d+R_e}{C_eR_dR_e} + \frac{1}{C_fR_e} + \frac{1}{C_dR_d}\right)\cdot\frac{d^2}{dt^2}v_n + \frac{C_d+C_e+C_f}{C_dC_eC_fR_dR_e}\cdot\frac{d}{dt}v_n = \frac{K\cdot v_n^2 - V_n}{C_dC_eC_fR_dR_eR_f}. \quad (14)$$

VII. BASINS OF ATTRACTION

All strange attractors presented in this paper that are either numerically integrated or experimentally observed belong to the class of self-excited. It means that close neighborhood of equilibria is a part of basin of attraction. However, searching for hidden attractors was not a subject of this paper. Thus, their existence is not entirely excluded from dynamics of analyzed mathematical models and can be revealed in future; more likely by application of apropos numerical algorithms rather than during experimental measurement.

Basins of the attraction were calculated for mathematical model (4) with and without resistor R_2. For the conservative case, achieved numerical results are provided by means of Fig. 20. Individual sub-spaces are slices defined by intervals $x \in (-0.1, 0.1)$ and $y =\in (-0.1, 0.1)$ in vertical direction; namely $z = -0.02$, $z = -0.01$, $z = 0$, $z = 0.01$, $z = 0.02$ and $z = 0.03$. Horizontal resolution is 10^{-4}. Note that basin

occupy very small state space volume while all other initial conditions pushes system toward infinity. However, close neighborhood of state space origin belongs to this object. On the other hand, dissipative system (4) exhibit large basin of the attraction for strange attractor as it is demonstrated in Fig. 21. Individual images are slices defined by intervals $x \in (-5, 5)$ and $y =\in (-5, 5)$ in vertical direction; namely beginning with $z = -2.2$ and ending with $z = 2.5$ with z-step 0.1 (that is total 48 planes). Horizontal resolution of these slices is 10^{-2}. For basin calculations, variable-step fourth-order integration method was utilized.

VIII. CONCLUSION AND DISCUSSION

This paper provides numerical analysis, circuit simulations and true experimental verification of the simplest possible configurations of fully analog chaotic oscillators with lumped parameters. Statement ''simplest possible'' seems to be strong proposition but it acts together with ''easy-to-be-constructed'' circuit feature simultaneously. By referring to fundamental structures of proposed chaotic oscillators, one resistor always serves for a voltage-to-current conversion. Thus, this element can be removed in the case of voltage-input current-output fourth-quadrant multiplier with the same transfer function. Such kind of device is not part of the market stocks currently. Considering this fact, third-order dissipative chaotic system cannot be constructed using less than three accumulation elements. Remaining resistor serves to set system dissipation in the case of non-conservative dynamics. Reduced amount of the circuit elements can result into non-solvable relations between mathematical model parameters (coefficients of the differential equation) and real-valued passive circuit elements (positive, non-extremal differences of the same kind).

Before starting design process, there were two preliminary design requirements only: utilization of one cheap and off-the-shelf active element and bifurcation scenario that can be controlled via change of the external DC voltage. Up to three circuit realizations were found which are different in the sense that there is no linear transformation of coordinates that transform one system to the other.

It is demonstrated that each designed chaotic oscillator represents jerky dynamics [113], [114]. Therefore, in these cases, algebraic simplicity turns also into circuit rusticity. Moreover, design method utilized in this work can be used for practical realization of the hyper-jerk dynamical systems. This approach can be adopted without modifications because in [115] some interesting quadratic cases were identified. The only difference is that a linear part of vector field will be constructed by using two biquadratic filters (can be passive) connected in cascade. Last but not least, some specific cases of hyper-chaotic systems can be considered as looped passive ladder filter and nonlinear active two-port as well. However, majority of 4D mathematical models can not be decomposed in such a way [116].

Each chaotic oscillator proposed in this paper is suitable for immediate design; both for educational purposes and as a core analog sub-circuit for the chaos-based communication platforms. It is because these provide structurally stable strange attractor having significantly large values of Kaplan-Yorke dimension $D_{KY} \approx 2.386$ comparable to the complex multi-wing attractors or the so-called labyrinth chaos with small dissipation [117], [118]. Next, our designed oscillators generate time domain waveforms with very good entropic properties. It means that segments of the output signals do not exhibit similar patterns. This feature can be tested by using several numerical approaches; for details and algorithms consult papers [119] and [120].

Despite of the strong effort chaotic behavior in circuit with RC ladder trans-impedance filter, i.e. parameter set leading to positive value of LLE, has not been detected so far. Probably, here we can find a place for future research.

Besides novel and very simple circuit topologies of the chaotic oscillators, where only one cheap four-quadrant analog multiplier is employed, this paper also brings rich overview of the research papers published in past twenty years. This work provides topics from the area of chaotic systems: shows multidisciplinary nature of chaos, describes design approach toward chaotic oscillators and mentions quantification methods of the chaotic dynamics.

REFERENCES

[1] T.-I. Chien and T.-L. Liao, ''Design of secure digital communication systems using chaotic modulation, cryptography and chaotic synchronization,'' *Chaos, Solitons Fractals*, vol. 24, no. 1, pp. 241–255, 2005. doi: 10.1016/j.chaos.2004.09.009.

[2] N. J. Corron and D. W. Hahs, ''A new approach to communications using chaotic signals,'' *IEEE Trans. Circuits Syst. I, Fundam. Theory Appl.*, vol. 44, no. 5, pp. 373–382, May 1997. doi: 10.1109/81.572333.

[3] M. Itoh, ''Spread spectrum communication via chaos,'' *Int. J. Chaos Theory Appl.*, vol. 9, no. 1, pp. 155–213, 1999. doi: 10.1142/S0218127499000080.

[4] E. N. Lorenz, ''Deterministic nonperiodic flow,'' *J. Atmos. Sci.*, vol. 20, no. 2, pp. 130–148, 1963. doi: 10.1175/1520-0469(1963)020.

[5] O. E. Rössler, ''Chemical turbulence: Chaos in a simple reaction-diffusion system,'' *J. Phys. Sci.*, vol. 31, no. 10, pp. 1168–1172, 1976. doi: 10.1515/zna-1976-1006.

[6] O. E. Rössler, ''An equation for continuous chaos,'' *Phys. Lett. A*, vol. 57, no. 5, pp. 397–398, 1976. doi: 10.1016/0375-9601(76)90101-8.

[7] R. Barrio, F. Blesa, and S. Serrano, ''Qualitative analysis of the Rössler equations: Bifurcations of limit cycles and chaotic attractors,'' *Phys. D, Nonlinear Phenomena*, vol. 238, no. 13, pp. 1087–1100, 2009. doi: 10.1016/j.physd.2009.03.010.

[8] S. I. Doumbouya, A. F. Muenster, J. C. Doona, and F. W. Schneider, ''Deterministic chaos in serially coupled chemical oscillators,'' *J. Phys. Chem.*, vol. 97, no. 5, pp. 1025–1031, 1993. doi: 10.1021/j100107a009.

[9] J. C. Doona, R. Blittersdorf, and F. W. Schneider, ''Deterministic chaos arising from homoclinicity in the chlorite-thiourea oscillator,'' *J. Phys. Chem.*, vol. 97, no. 28, pp. 7258–7263, 1993. doi: 10.1021/j100130a023.

[10] P. Bo, V. Petrov, and K. Showalter, ''Controlling chemical chaos,'' *J. Phys. Chem.*, vol. 95, no. 13, pp. 4957–4959, 1991. doi: 10.1021/j100166a013.

[11] Y. Kuramoto and T. Yamada, ''Turbulent state in chemical reactions,'' *Progr. Theor. Theor. Phys.*, vol. 56, no. 2, pp. 679–681, 1976. doi: 10.1143/PTP.56.679.

[12] D. Ruelle and F. Takens, ''On the nature of turbulence,'' *Commun. Math. Phys.*, vol. 20, no. 3, pp. 167–192, 1971. doi: 10.1007/BF01646553.

[13] H. A. Posch, W. O. Hoover, and F. J. Vesely, ''Canonical dynamics of the Nosé oscillator: Stability, order, and chaos,'' *Phys. Rev. A, Gen. Phys.*, vol. 33, no. 6, pp. 4253–4265, 1986. doi: 10.1103/PhysRevA.33.4253.

[14] Y. Ueda, ''Randomly transitional phenomena in the system governed by Duffing's equation,'' *J. Stat. Phys.*, vol. 20, no. 2, pp. 181–196, 1979. doi: 10.1007/BF01011512.

[15] T. Kousaka, H. Asahara, and N. Inaba, "Stick–slip chaos in a mechanical oscillator with dry friction," *Prog. Theor. Experim. Phys.*, vol. 2018, no. 3, pp. 1–20, 2018. doi: 10.1093/ptep/pty016.

[16] E. H. Dowell, "Chaotic oscillations in mechanical systems," *Comput. Struct.*, vol. 30, nos. 1–2, pp. 171–184, 1988. doi: 10.1016/0045-7949(88)90225-8.

[17] B. Błażejczyk, T. Kapitaniak, J. Wojewoda, and J. Brindley, "Controlling chaos in mechanical systems," *Appl. Mech. Rev.*, vol. 46, no. 7, pp. 385–391, 1993. doi: 10.1115/1.3120367.

[18] J. P. Singh, K. Lochan, N. V. Kuznetsov, and B. K. Roy, "Coexistence of single- and multi-scroll chaotic orbits in a single-link flexible joint robot manipulator with stable spiral and index-4 spiral repellor types of equilibria," *Nonlinear Dyn.*, vol. 90, no. 2, pp. 1277–1299, 2017. doi: 10.1007/s11071-017-3726-4.

[19] R. M. May *et al.*, "Chaos and the dynamics of biological populations," *Proc. Roy. Soc. A, Math. Phys. Eng. Sci.*, vol. 413, no. 2, pp. 207–230, 2001. doi: 10.1098/rspa.1987.0098.

[20] R. Dilão and T. Domingos, "Periodic and quasi-periodic behavior in resource-dependent age structured population models," *Bull. Math. Biol.*, vol. 63, no. 2, pp. 207–230, 2001. doi: 10.1006/bulm.2000.0213.

[21] S. Narayanan and K. Jayaraman, "Chaotic oscillations of a square prism in fluid flow," *J. Sound Vib.*, vol. 166, no. 1, pp. 87–101, 1993. doi: 10.1006/jsvi.1993.1285.

[22] M. P. Païdoussis and F. C. Moon, "Nonlinear and chaotic fluidelastic vibrations of a flexible pipe conveying fluid," *J. Fluids Struct.*, vol. 2, no. 6, pp. 567–591, 1988. doi: 10.1016/S0889-9746(88)80023-9.

[23] D. Y. Hsieh, "Hydrodynamic instabilty, chaos and phase transition," *Nonlinear Anal., Theory, Methods Appl.*, vol. 30, no. 8, pp. 5327–5334, 1997. doi: 10.1016/S0362-546X(96)00151-4.

[24] T. Nagatani, "Chaotic jam and phase transition in traffic flow with passing," *Phys. Rev. E, Stat. Phys. Plasmas Fluids Relat. Interdiscip. Top.*, vol. 60, no. 2, pp. 1535–1541, 1999. doi: 10.1103/PhysRevE.60.1535.

[25] T. Li, "Nonlinear dynamics of traffic jams," *Phys. D, Nonlinear Phenom.*, vol. 207, nos. 1–2, pp. 41–51, 2005. doi: 10.1016/j.physd.2005.05.011.

[26] J. Gu and S. Chen, "Nonlinear analysis on traffic flow based on catastrophe and chaos theory," *Discrete Dyn. Nature Soc.*, vol. 2014, Nov. 2014, Art. no. 535167. doi: 10.1155/2014/535167.

[27] P. Shang, X. Li, and S. Kamae, "Chaotic analysis of traffic time series," *Chaos, Solitons Fractals*, vol. 25, pp. 121–128, Jul. 2005. doi: 10.1016/j.chaos.2004.09.104.

[28] A. Babloyantz, J. M. Salazar, and C. Nicolis, "Evidence of chaotic dynamics of brain activity during the sleep cycle," *Phys. Lett. A*, vol. 111, no. 3, pp. 152–156, 1985. doi: 10.1016/0375-9601(85)90444-X.

[29] B. B. Ferreira, A. S. de Paula, and M. A. Savi, "Chaos control applied to heart rhythm dynamics," *Chaos, Solitons Fractals*, vol. 44, no. 8, pp. 587–599, 2011. doi: 10.1016/j.chaos.2011.05.009.

[30] X. Wang, J. Meng, G. Tan, and L. Zou, "Research on the relation of EEG signal chaos characteristics with high-level intelligence activity of human brain," *Nonlinear Biomed. Phys.*, vol. 4, no. 2, pp. 1–20, 2010. doi: 10.1186/1753-4631-4-2.

[31] M. Itoh, "Synthesis of electronic circuits for simulating nonlinear dynamics," *Int. J. Bifurcation Chaos*, vol. 11, no. 3, pp. 605–653, 2001. doi: 10.1142/S0218127401002341.

[32] J. Petržela, Z. Hruboš, and T. Gotthans, "Modeling deterministic chaos using electronic circuits," *Radioengineering*, vol. 20, no. 2, pp. 438–444, 2011.

[33] T. Götthans and J. Petržela, "Experimental study of the sampled labyrinth chaos," *Radioengineering*, vol. 20, no. 4, pp. 873–879, 2011.

[34] J. Petržela, T. Gotthans, and M. Guzan, "Current-mode network structures dedicated for simulation of dynamical systems with plane continuum of equilibrium," *J. Circuits, Syst. Comput.*, vol. 27, no. 9, p. 1830004, 2018. doi: 10.1142/S0218126618300040.

[35] A. S. Elwakil and M. P. Kennedy, "Chaotic oscillator configuration using a frequency dependent negative resistor," *J. Circuits, Syst. Comput.*, vol. 9, no. 3, pp. 229–242, 1999. doi: 10.1142/S0218126699000190.

[36] L. O. Chua and G. N. Lin, "Canonical realization of Chua's circuit family," *IEEE Trans. Circuit Syst.*, vol. 37, no. 7, pp. 885–902, Jul. 1990. doi: 10.1109/31.55064.

[37] A. S. Elwakil and M. P. Kennedy, "A semi-systematic procedure for producing chaos from sinusoidal oscillators using diode-inductor and FET-capacitor composites," *IEEE Trans. Circuits Syst. I, Fundam. Theory Appl.*, vol. 47, no. 4, pp. 582–590, Apr. 2000. doi: 10.1109/81.841862.

[38] A. S. Elwakil and M. P. Kennedy, "Novel chaotic oscillator configuration using a diode-inductor composite," *Int. J. Circuit Theory Appl.*, vol. 87, no. 4, pp. 397–406, 2010. doi: 10.1080/002072100132057.

[39] M. P. Kennedy, "Robust OP AMP realization Of Chua's circuit," *Frequenz*, vol. 46, nos. 3–4, pp. 66–80, 1992. doi: 10.1515/FREQ.1992.46.3-4.66.

[40] R. Tokunaga, M. Komuro, T. Matsumoto, and L. O. Chua, "'Lorenz attractor' from an electrical circuit with uncoupled continuous piecewise-linear resistor," *Int. J. Circuit Theory Appl.*, vol. 17, no. 1, pp. 71–85, 1989. doi: 10.1002/cta.4490170108.

[41] S. Ozoguz and N. S. Sengor, "On the realization of NPN-only log-domain chaotic oscillators," *IEEE Trans. Circuits Syst. I, Fundam. Theory Appl.*, vol. 50, no. 2, pp. 291–294, Feb. 2003. doi: 10.1109/TCSI.2002.808230.

[42] R. Trejo-Guerra, E. Tlelo-Cuautle, V. H. Cabajal-Gómez, and G. Rodriguez-Gómez, "A survey on the integrated design of chaotic oscillators," *Appl. Math. Comput.*, vol. 219, no. 10, pp. 5113–5122, 2013. doi: 10.1016/j.amc.2012.11.021.

[43] Ş. Ç. Yener and H. H. Kuntman, "Fully CMOS memristor based chaotic circuit," *Radioengineering*, vol. 23, no. 4, pp. 1140–1149, 2014.

[44] T. Stojanovski, J. Pihl, and L. Kocarev, "Chaos-based random number generators. Part II: Practical realization," *IEEE Trans. Circuits Syst. I, Fundam. Theory Appl.*, vol. 48, no. 3, pp. 382–385, Mar. 2001. doi: 10.1109/81.915396.

[45] M. Drutarovsky and P. Galajda, "A robust chaos-based true random number generator embedded in reconfigurable switched-capacitor hardware," *Radioengineering*, vol. 16, no. 3, pp. 120–127, 2007.

[46] G. Kaddoum, "Wireless chaos-based communication systems: A comprehensive survey," *IEEE Access*, vol. 4, pp. 2621–2648, 2016. doi: 10.1109/ACCESS.2016.2572730.

[47] L.-F. Zhang, X.-L. An, and J. Zhang, "A new chaos synchronization scheme and its application to secure communications," *Nonlinear Dyn.*, vol. 73, pp. 705–722, Jul. 2013. doi: 10.1007/s11071-013-0824-9.

[48] N. Jia and T. Wang, "Chaos control and hybrid projective synchronization for a class of new chaotic systems," *Comput. Math. Appl.*, vol. 62, no. 12, pp. 4783–4795, 2011. doi: 10.1016/j.camwa.2011.10.069.

[49] X. S. Yang and Q. Li, "Chaos generator via Wien-bridge oscillator," *Electron. Lett.*, vol. 38, no. 13, pp. 623–625, Jun. 2002. doi: 10.1049/el:20020456.

[50] R. Kiliç and F. Yildirim, "A survey of Wien bridge-based chaotic oscillators: Design and experimental issues," *Chaos, Solitons Fractals*, vol. 38, no. 5, pp. 1394–1410, 2008. doi: 10.1016/j.chaos.2008.02.016.

[51] O. Morgul, "Wien bridge based RC chaos generator," *Electron. Lett.*, vol. 31, no. 24, pp. 2058–2059, Nov. 1995. doi: 10.1049/el:19951411.

[52] M. P. Kennedy, "Chaos in the Colpitts oscillator," *IEEE Trans. Circuits Syst. I, Fundam. Theory Appl.*, vol. 41, no. 11, pp. 771–774, Nov. 1994. doi: 10.1109/81.331536.

[53] K. Peter, "Chaos in Hartley's oscillator," *Int. J. Bifurcation Chaos*, vol. 12, no. 10, pp. 2229–2232, 2002. doi: 10.1142/S0218127402005777.

[54] J. Petržela, "On the existence of chaos in the electronically adjustable structures of the state variable filters," *Int. J. Circuit Theory Appl.*, vol. 44, no. 10, pp. 1779–1797, 2016. doi: 10.1002/cta.2193.

[55] H. H. C. Lu, D. S. Yu, A. L. Fitch, V. Sreeram, and H. Chen, "Controlling chaos in a memristor based circuit using a twin-T notch filter," *IEEE Trans. Circuits Syst. I, Reg. Papers*, vol. 58, no. 6, pp. 1337–1344, Jun. 2011. doi: 10.1109/TCSI.2010.2097771.

[56] J. Petržela, "Chaotic behaviour of state variable filters with saturation-type integrators," *Electron. Lett.*, vol. 51, no. 15, pp. 1159–1161, 2015. doi: 10.1049/el.2015.1563.

[57] E. Fossas and G. Olivar, "Study of chaos in the buck converter," *IEEE Trans. Circuits Syst. I, Fundam. Theory Appl.*, vol. 43, no. 1, pp. 13–25, Jan. 1996. doi: 10.1109/91.481457.

[58] C. K. Tse and W. C. Y. Chan, "Chaos from a current-programmed ĆUK converter," *Int. J. Circuit Theory Appl.*, vol. 23, no. 3, pp. 217–225, 1995. doi: 10.1002/cta.4490230304.

[59] D. Pikulin, "Subharmonic oscillations and chaos in DC-DC switching converters," *Elektron. Elektrotechn.*, vol. 19, no. 4, pp. 33–36, 2013. doi: 10.5755/j01.19.4.4054.

[60] J. H. B. Deane, "Chaos in a current-mode controlled boost DC-DC converter," *IEEE Trans. Circuits Syst. I, Fundam. Theory Appl.*, vol. 39, no. 8, pp. 680–683, Aug. 1992. doi: 10.1109/81.168922.

[61] X. Zhou, J. Li, and Y. Ma, "Chaos phenomena in DC-DC converter and chaos control," *Procedia Eng.*, vol. 29, no. 12, pp. 470–473, 2012. doi: 10.1016/j.proeng.2011.12.744.

[62] M. di Bernardo, F. Garefalo, L. Glielmo, and F. Vasca, "Switchings, bifurcations, and chaos in DC/DC converters," *IEEE Trans. Circuits Syst. I, Fundam. Theory Appl.*, vol. 45, no. 2, pp. 133–141, Feb. 1998. doi: 10.1109/81.661675.

[63] D. C. Hamill and D. J. Jeffries, "Subharmonics and chaos in a controlled switched-mode power converter," *IEEE Trans. Circuits Syst.*, vol. 35, no. 8, pp. 1059–1061, Aug. 1988. doi: 10.1109/31.1858.

[64] D. Dai, X. Ma, B. Zhang, and C. K. Tse, "Hopf bifurcation and chaos from torus breakdown in voltage-mode controlled DC drive systems," *Chaos, Solitons Fractals*, vol. 41, no. 2, pp. 1027–1033, 2009. doi: 10.1016/j.chaos.2008.04.053.

[65] A. Rodriguez-Vazquez, J. Huertas, and L. Chua, "Chaos in switched-capacitor circuit," *IEEE Trans. Circuits Syst.*, vol. 32, no. 10, pp. 1083–1085, Oct. 1985. doi: 10.1109/TCS.1985.1085626.

[66] C. K. Tse, "Flip bifurcation and chaos in three-state boost switching regulators," *IEEE Trans. Circuits Syst. I, Fundam. Theory Appl.*, vol. 41, no. 1, pp. 16–23, Jan. 1994. doi: 10.1109/TCS.1985.1085626.

[67] Z. T. Zhusubaliyev, E. Mosekilde, V. G. Rubanov, and R. A. Nabokov, "Multistability and hidden attractors in a relay system with hysteresis," *Phys. D, Nonlinear Phenomena*, vol. 306, pp. 6–15, Jun. 2015. doi: 10.1016/j.physd.2015.05.005.

[68] T. Endo and L. O. Chua, "Chaos from phase-locked loops," *IEEE Trans. Circuits Syst.*, vol. 35, no. 8, pp. 987–1003, Aug. 1988. doi: 10.1109/31.1845.

[69] T. Endo, "A review of chaos and nonlinear dynamics in phase-locked loops," *J. Franklin Inst.*, vol. 331, no. 6, pp. 859–902, 1994. doi: 10.1016/0016-0032(94)90091-4.

[70] M. Beyki and M. Yaghoobi, "Chaotic logic gate: A new approach in set and design by genetic algorithm," *Chaos, Solitons Fractals*, vol. 77, no. 5, pp. 247–252, 2015. doi: 10.1016/j.chaos.2015.05.032.

[71] J. Petržela, "Multi-valued static memory with resonant tunneling diodes as natural source of chaos," *Nonlinear Dyn.*, vol. 94, no. 3, pp. 1867–1887, 2018. doi: 10.1007/s11071-018-4462-0.

[72] J. Petržela, "Strange attractors generated by multiple-valued static memory cell with polynomial approximation of resonant tunneling diodes," *Entropy*, vol. 20, no. 9, p. 697, 2018. doi: 10.3390/e20090697.

[73] P. Bartissol and L. O. Chua, "The double hook (nonlinear chaotic circuits)," *IEEE Trans. Circuits Syst.*, vol. 35, no. 12, pp. 1512–1522, Dec. 1988. doi: 10.1109/31.9914.

[74] J. C. Sprott, S. Jafari, V.-T. Pham, and Z. S. Hosseini, "A chaotic system with a single unstable node," *Phys. Lett. A*, vol. 379, no. 36, pp. 2030–2036, 2015. doi: 10.1016/j.physleta.2015.06.039.

[75] X. Wang and G. Chen, "A chaotic system with only one stable equilibrium," *Commun. Nonlinear Sci. Numer. Simul.*, vol. 17, no. 3, pp. 1264–1272, 2012. doi: 10.1016/j.cnsns.2011.07.017.

[76] X. Wang, V.-T. Pham, S. Jafari, C. Volos, J. M. Munoz-Pacheco, and E. Tlelo-Cuautle, "A new chaotic system with stable equilibrium: From theoretical model to circuit implementation," *IEEE Access*, vol. 5, pp. 8851–8857, 2017. doi: 10.1109/ACCESS.2017.2693301.

[77] Z. Wei and Q. Yang, "Dynamical analysis of the generalized Sprott C system with only two stable equilibria," *Nonlinear Dyn.*, vol. 68, no. 4, pp. 543–554, 2012. doi: 10.1007/s11071-011-0235-8.

[78] Q. Yang, Z. Wei, and G. Chen, "An unusual 3D autonomous quadratic chaotic system with two stable node-foci," *Int. J. Bifurcation Chaos*, vol. 20, no. 4, pp. 1061–1083, 2010. doi: 10.1142/S0218127410026320.

[79] Q. Yang and G. Chen, "A chaotic system with one saddle and two stable node-foci," *Int. J. Bifurcation Chaos*, vol. 18, no. 5, pp. 1393–1414, 2008. doi: 10.1142/S0218127408021063.

[80] J. P. Singh and B. K. Roy, "Crisis and inverse crisis route to chaos in a new 3-D chaotic system with saddle, saddle foci and stable node foci nature of equilibria," *Optik*, vol. 127, no. 24, pp. 11982–12002, 2016. doi: 10.1016/j.ijleo.2016.09.107.

[81] V.-T. Pham, C. Volos, S. Jafari, Z. Wei, and X. Wang, "Constructing a novel no-equilibrium chaotic system," *Int. J. Bifurcation Chaos*, vol. 24, no. 5, p. 1450073, 2014. doi: 10.1142/S0218127414500734.

[82] X. Wang and G. Chen, "Constructing a chaotic system with any number of equilibria," *Nonlinear Dyn.*, vol. 71, no. 3, pp. 429–436, 2013. doi: 10.1007/s11071-012-0669-7.

[83] S. Mobayen, C. K. Volos, S. Kaçar, U. Çavuşoğlu, and B. Vaseghi, "A chaotic system with infinite number of equilibria located on an exponential curve and its chaos-based engineering application," *Int. J. Bifurcation Chaos*, vol. 28, no. 9, p. 1850112, 2018. doi: 10.1142/S0218127418501122.

[84] S. Jafari and J. C. Sprott, "Simple chaotic flows with a line equilibrium," *Chaos, Solitons Fractals*, vol. 57, no. 8, pp. 79–84, 2013. doi: 10.1016/j.chaos.2013.08.018.

[85] J. P. Singh and B. K. Roy, "The simplest 4-D chaotic system with line of equilibria, chaotic 2-torus and 3-torus behavior," *Nonlinear Dyn.*, vol. 89, no. 3, pp. 1845–1862, 2017. doi: 10.1007/s11071-017-3556-4.

[86] J. Petržela and T. Gotthans, "New chaotic dynamical system with a conic-shaped equilibrium located on the plane structure," *Appl. Sci.*, vol. 7, no. 10, p. 976, 2017. doi: 10.3390/app7100976.

[87] T. Gotthans and J. Petržela, "New class of chaotic systems with circular equilibrium," *Nonlinear Dyn.*, vol. 81, no. 3, pp. 1143–1149, 2015. doi: 10.1007/s11071-015-2056-7.

[88] T. Gotthans, J. C. Sprott, and J. Petržela, "Simple chaotic flow with circle and square equilibrium," *Int. J. Bifurcation Chaos*, vol. 26, no. 8, p. 1650137, 2016. doi: 10.1142/S0218127416501376.

[89] K. Barati, S. Jafari, J. C. Sprott, and V.-T. Pham, "Simple chaotic flows with a curve of equilibria," *Int. J. Bifurcation Chaos*, vol. 26, no. 12, p. 1630034, 2016. doi: 10.1142/S0218127416300342.

[90] S. Jafari, J. C. Sprott, and M. Molaie, "A simple chaotic flow with a plane of equilibria," *Int. J. Bifurcation Chaos*, vol. 26, no. 6, p. 1650098, 2016. doi: 10.1142/S021812741650098X.

[91] S. Jafari, J. C. Sprott, V.-T. Pham, C. Volos, and CH. Li, "Simple chaotic 3D flows with surfaces of equilibria," *Nonlinear Dyn.*, vol. 86, no. 2, pp. 1349–1358, 2016. doi: 10.1007/s11071-016-2968-x.

[92] V.-T. Pham, S. Jafari, C. Volos, and T. Kapitaniak, "Different families of hidden attractors in a new chaotic system with variable equilibrium," *Int. J. Bifurcation Chaos*, vol. 27, no. 9, p. 1750138, 2017. doi: 10.1142/S0218127417501383.

[93] J. C. Sprott, "Some simple chaotic jerk functions," *Amer. J. Phys.*, vol. 65, no. 6, pp. 537–543, 1997. doi: 10.1119/1.18585.

[94] J. C. Sprott, "Simplest dissipative chaotic flow," *Phys. Lett. A*, vol. 228, nos. 4–5, pp. 271–274, 1997. doi: 10.1016/S0375-9601(97)00088-1.

[95] J. C. Sprott and S. J. Linz, "Algebraically simple chaotic flows," *Int. J. Chaos Theory Appl.*, vol. 5, no. 2, pp. 3–22, 2000.

[96] J. C. Sprott, "Some simple chaotic flows," *Phys. Rev. E, Stat. Phys. Plasmas Fluids Relat. Interdiscip. Top.*, vol. 50, no. 2, pp. 647–650, 1994. doi: 10.1103/PhysRevE.50.R647.

[97] B. Munmuangsaen, B. Srisuchinwong, and J. C. Sprott, "Generalization of the simplest autonomous chaotic system," *Phys. Lett. A*, vol. 375, no. 12, pp. 1445–1450, 2011. doi: 10.1016/j.physleta.2011.02.028.

[98] J. P. Singh and B. K. Roy, "Second order adaptive time varying sliding mode control for synchronization of hidden chaotic orbits in a new uncertain 4-D conservative chaotic system," *Trans. Inst. Meas. Control*, vol. 40, no. 13, pp. 3573–3586, 2017. doi: 10.1177/0142331217727580.

[99] G.-Q. Zhong, K.-T. Ko, K.-F. Man, and K.-S. Tang, "A systematic procedure for synthesizing two-terminal devices with polynomial nonlinearity," *Int. J. Circuit Theory Appl.*, vol. 29, no. 2, pp. 241–249, 2001. doi: 10.1002/cta.141.

[100] J. Petržela and V. Pospíšil, "Nonlinear resistor with polynomial AV characteristics and its application in chaotic oscillator," *Radioengineering*, vol. 13, no. 2, pp. 20–25, 2004.

[101] B. Muthuswamy and L. O. Chua, "Simplest chaotic circuit," *Int. J. Bifurcation Chaos*, vol. 20, no. 5, pp. 1567–1580, 2010. doi: 10.1142/S0218127410027076.

[102] Z. Biolek, D. Biolek, and V. Biolkova, "Differential equations of ideal memristors," *Radioengineering*, vol. 24, no. 2, pp. 369–377, 2015. doi: 10.13164/re.2015.0369.

[103] Z. Biolek and D. Biolek, "Euler-Lagrange equations of networks with higher-order elements," *Radioengineering*, vol. 26, no. 2, pp. 397–405, 2017. doi: 10.13164/re.2017.0397.

[104] G.-Q. Zhong, "Implementation of Chua's circuit with a cubic nonlinearity," *IEEE Trans. Circuits Syst. I, Fundam. Theory Appl.*, vol. 41, no. 12, pp. 934–941, 1994. doi: 10.1109/81.340866.

[105] S. Jafari, J. C. Sprott, V.-T. Pham, and S. M. R. H. Golpayegani, "A new cost function for parameter estimation of chaotic systems using return maps as fingerprints," *Int. J. Bifurcation Chaos*, vol. 24, no. 10, p. 1450134, 2014. doi: 10.1142/S0218127410027076.

[106] J. Petržela, "Optimal piecewise-linear approximation of the quadratic chaotic dynamics," *Radioengineering*, vol. 21, no. 1, pp. 20–28, 2012.
[107] H. P. W. Gottlieb and J. C. Sprott, "Simplest driven conservative chaotic oscillator," *Phys. Lett. A*, vol. 291, no. 6, pp. 385–388, 2001. doi: 10.1016/S0375-9601(01)00765-4.
[108] J. Petržela and J. Slezák, "Conservative chaos generators with CCII+ based on mathematical model of nonlinear oscillator," *Radioengineering*, vol. 17, no. 3, pp. 19–24, 2008.
[109] M. J. Ogorzalek, "Order and chaos in a third-order RC ladder network with nonlinear feedback," *IEEE Trans. Circuits Syst.*, vol. 36, no. 9, pp. 1221–1230, Sep. 1989. doi: 10.1109/31.34668.
[110] P. Bernat and I. Balaz, "RC autonomous circuits with chaotic behaviour," *Radioengineering*, vol. 11, no. 2, pp. 1–5, 2002.
[111] S. Panahi, S. Jafari, V.-T. Pham, S. T. Kingni, A. Zahedi, and S. H. Sedighy, "Parameter identification of a chaotic circuit with a hidden attractor using Krill Herd optimization," *Int. J. Bifurcation Chaos*, vol. 26, no. 13, p. 1650221, 2016, 10.1142/S0218127416502217.
[112] A. Wolf, J. B. Swift, H. L. Swinney, and J. A. Vastano, "Determining Lyapunov exponents from a time series," *Phys. D, Nonlinear Phenomena*, vol. 16, no. 3, pp. 285–317, 1985. doi: 10.1016/0167-2789(85)90011-9.
[113] J. Petržela, Z. Kolka, and S. Hanus, "Simple chaotic oscillator: From mathematical model to practical experiment," *Radioengineering*, vol. 15, no. 1, pp. 6–12, 2006.
[114] L. Chunxia, Y. Jie, X. Xiangchun, A. Limin, Q. Yan, and F. Yongqing, "Research on the multi-scroll chaos generation based on jerk mode," *Proceedia Eng.*, vol. 29, pp. 957–961, 2012. doi: 10.1016/j.proeng.2012.01.071.
[115] K. E. Chlouverakis and J. C. Sprott, "Chaotic hyperjerk systems," *Chaos, Solutions Fractals*, vol. 28, no. 3, pp. 739–746, May 2006. doi: 10.1016/j.chaos.2005.08.019.
[116] J. P. Singh and B. K. Roy, "Hidden attractors in a new complex generalised Lorenz hyperchaotic system, its synchronisation using adaptive contraction theory, circuit validation and application," *Nonlinear Dyn.*, vol. 92, no. 2, pp. 373–394, 2018. doi: 10.1007/s11071-018-4062-z.
[117] J. C. Sprott and K. E. Chlouverakis, "Labyrinth chaos," *Int. J. Bifurcation Chaos*, vol. 17, no. 6, pp. 2097–2108, 2007. doi: 10.1142/S0218127407018245.
[118] K. E. Chlouverakis and J. C. Sprott, "Hyperlabyrinth chaos: From chaotic walks to spatiotemporal chaos," *Chaos*, vol. 17, Sep. 2007, Art. no. 023110. doi: 10.1063/1.2721237.
[119] G. Györgyi and P. Szépfalusy, "Calculation of the entropy in chaotic systems," *Phys. Rev. A, Gen. Phys.*, vol. 31, pp. 3477–3479, May 1985. doi: 10.1103/PhysRevA.313477.
[120] T. Kapitaniak, S. A. Mohammadi, S. Mekhilef, F. E. Alsaadi, T. Hayat, and V.-T. Pham, "A new chaotic system with stable equilibrium: Entropy analysis, parameter estimation, and circuit design," *Entropy*, vol. 20, no. 9, p. 670, 2018. doi: 10.3390/e20090670.

JIRI PETRZELA was born in Brno, Czech Republic, in 1978. He received the M.Sc. and Ph.D. degrees in the field of theoretical electronics, in 2003 and 2007, respectively. He is currently an Associate Professor with the Department of Radio Electronics, Faculty of Electrical Engineering and Communications, Brno University of Technology, Czech Republic. He is a main author or co-author of more than 20 journal papers and 40 international conference contributions. His research interests include numerical methods in electrical engineering, nonlinear dynamics, chaos theory, analog lumped circuit design, and computer-aided analysis.

LADISLAV POLAK was born in Štúrovo, Slovakia, in 1984. He received the M.Sc. and Ph.D. degrees in electronics and communication from the Brno University of Technology, Czech Republic, in 2009 and 2013, respectively, where he is currently an Associate Professor with the Department of Radio Electronic. His research interests include wireless communication systems, RF measurement, signal processing, and computer-aided analysis. He has been a member of the IEEE, since 2010. He has been an Associate Editor of the *Radioengineering* journal, since 2013.